

# Deriving mesoscopic models of collective behaviour for finite populations

Jitesh Jhavar<sup>1</sup>, Richard G. Morris<sup>2</sup>, Vishwesh Guttal<sup>1</sup>

1. Centre for Ecological Sciences, Indian Institute of Science, Bengaluru, 560012

2. National Centre for Biological Sciences, TIFR, Bengaluru, 560012

---

## Abstract

Animal groups exhibit many emergent properties that are a consequence of local interactions. Linking individual-level behaviour, which is often stochastic and local, to coarse-grained descriptions of animal groups has been a question of fundamental interest from both biological and mathematical perspectives. In this book chapter, we present two complementary approaches to derive *coarse-grained* descriptions of collective behaviour at so-called *mesoscopic* scales, which account for the stochasticity arising from the finite sizes of animal groups. We construct stochastic differential equations (SDEs) for a coarse-grained variable that describes the order/consensus within a group. The first method of construction is based on van Kampen's system-size expansion of transition rates. The second method employs Gillespie's chemical Langevin equations. We apply these two methods to two *microscopic* models from the literature, in which organisms stochastically interact and choose between two directions/choices of foraging. These 'binary-choice' models differ only in the types of interactions between individuals, with one assuming simple pairwise interactions, and the other incorporating ternary effects. In both cases, the derived mesoscopic SDEs have multiplicative/state-dependent noise, *i.e.*, the strength of the noise depends on the current state of the system. However, the different models demonstrate the contrasting effects of noise: *increasing* the order/consensus in the pairwise interaction model, whilst *reducing* the order/consensus in the higher-order interaction model. We verify the validity of such mesoscopic behaviour by numerical simulations of the underlying microscopic models. Although both methods yield identical SDEs for *binary-choice* systems that are effectively one-dimensional, the relative tractability of the chemical Langevin approach is beneficial in generalizations to higher-dimensions. We hope that this book chapter provides a pedagogical review of two complementary methods to construct mesoscopic descriptions from microscopic rules, how the noise in mesoscopic models is often multiplicative/state-dependent, and finally, how such noise can have counter-intuitive effects on shaping collective behaviour.

---

*keywords: demographic noise, multiplicative noise, nonlinear dynamics, Fokker-Planck equation, Langevin equation, noise-induced transitions, ecology, collective motion, population dynamics, collective decision making*

## 1. Introduction

Collective behaviour is widespread in the animal kingdom, where many properties of animal groups are emergent, *i.e.*, they often arise from simple local interactions among individuals (Vicsek et al., 1995; Couzin et al., 2002; Parrish et al., 2002; Sumpter, 2010, 2006). These emergent properties include, for example, visually fantastic patterns of flocks of starlings swirling in synchrony (Cavagna et al., 2010; Attanasi et al., 2014), locusts on the march (Uvarov, 1977; Simpson and Sword, 2008; Buhl et al., 2006), conflict resolution and consensus decision making in

groups of animals (Deneubourg and Goss, 1989; Petit and Bon, 2010; Beckers et al., 1990; Pratt et al., 2002; Couzin et al., 2005), collective navigation (Grünbaum, 1998; Guttal and Couzin, 2010; Berdahl et al., 2013), or colonies of social insects performing complex tasks (Seeley, 1989; Franks et al., 1992; Dussutour et al., 2006; Schultheiss and Cheng, 2012; Gordon, 1996; Bonabeau et al., 1997).

Understanding these emergent properties has proved to be a topic of great interest in both biology and the physical sciences (Flierl et al., 1999; Camazine et al., 2003; Sumpter, 2010; Guttal, 2014). Broadly speaking, the focus of biologists has typically been to understand how organisms interact; processing local information from their neighbours. This information is often noisy and inaccurate, yet repeated interactions amongst individuals can result in the aforementioned collective properties. Physicists and mathematicians, by contrast, have tried to develop simple theories to describe how local interactions between such agents can combine to result in larger scale properties of groups and populations. These two approaches are almost complementary to each other, with theory able to make connections between the observed meso/macroscale behaviours and the likely individual-level decisions of organisms; the latter being difficult to measure directly in the natural setting of a group.

Here, we will use the word *microscopic* to refer to behaviour at the individual level ( $N = 1$ ), and the word *macroscopic* to describe the behaviour of infinite sized systems ( $N \rightarrow \infty$ ). The *mesoscopic* scale is in between these two, and corresponds to intermediate (large but finite) group sizes. The aim of this book chapter is to introduce readers to a couple of complementary analytical methods that help us link individual behaviour to emergent properties of the collective. In doing so, our focus will be on the mesoscopic scale: aiming to understand the important role of stochasticity resulting from finite group sizes.

## 2. Background

For historical context, we begin by briefly presenting the classic *Vicsek model* of collective motion (Vicsek et al., 1995), which has had a profound impact on the field of collective behavior. It has inspired a large body of theoretical and empirical research in physics, mathematics and biology. In this simple model, we consider a population of  $N$  self-propelled particles (SPP) moving with constant speed  $s$  in a continuous space of volume  $L^d$ , where  $d$  is the spatial dimension. (For the purpose of this chapter we restrict ourselves to one- and two-dimensions only). Boundary conditions are assumed to be periodic, implying that a particle leaving the boundary at the right-extreme returns to the left-extreme edge of the space, *etc.* Topologically, a one-dimensional system with periodic boundaries is equivalent to a ring whereas a two-dimensional system is equivalent to a torus.

The basic rule of the model is that each individual,  $i$ , moves in the average direction of its *neighbors*, plus some small error. More specifically, at any given time  $t$ , the directions of all individuals  $\{\theta_i : i = 1, \dots, N\}$  are updated synchronously according to

$$\theta_i(t + \delta t) = \overline{\theta(t)} + \Delta\theta(t), \tag{1}$$

where the overbar represents an average over individuals within a radius  $r$  from the location of individual  $i$ , the so-called *focal* individual. The first term on the right-hand side captures how the focal individual responds to interactions with its neighbours, and corresponds to calculating  $\arctan(\overline{\sin\theta}/\overline{\cos\theta})$ . The second term is a noise term representing the error a focal individual makes while copying the average neighborhood direction.  $\Delta\theta(t)$  is therefore a random variable, typically chosen from a uniform distribution over the range  $[-\eta/2, \eta/2]$ , where  $\eta \leq 2\pi$ . Once the directions

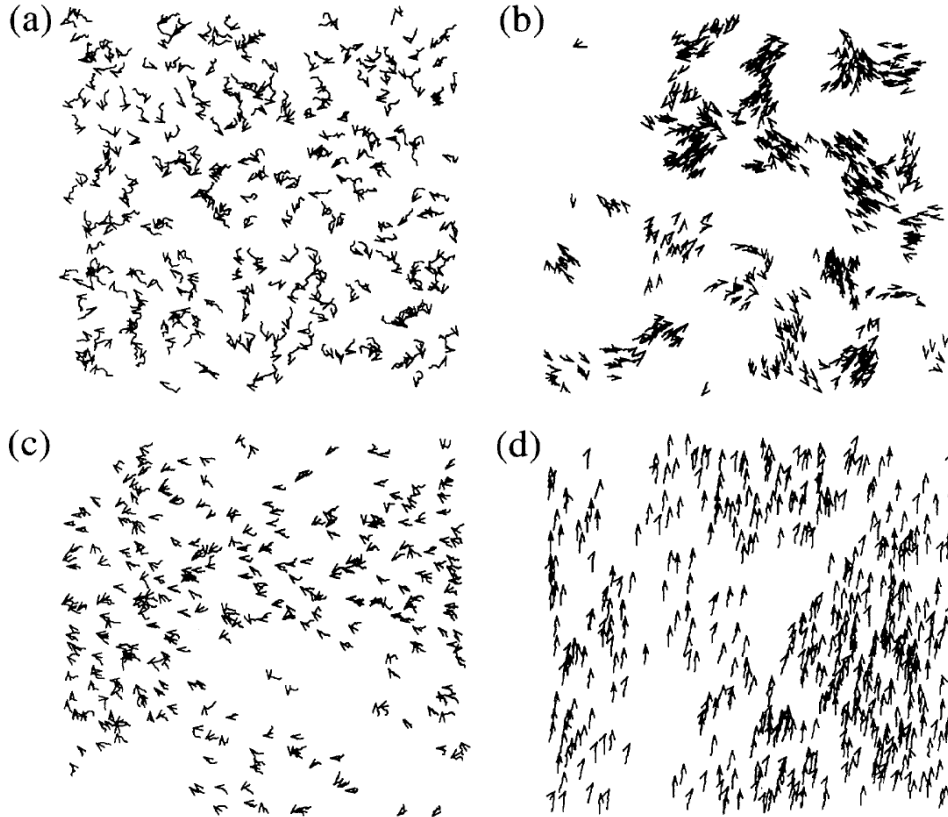


Figure 1: Various patterns of collective motion produced by the classic Vicsek model of collective motion. Reproduced here with permission from *American Physical Society: Physical Review Letters* (Vicsek et al., 1995). There are 300 particles in each of these panels, with the arrow indicating the current direction of motion and the short solid lines preceding it indicates the trajectory of that particle over last 20 time steps. (a) High density and large-noise ( $L = 7$ ,  $\eta = 2.0$ ), but initial stages of simulation. (b) Low-density and low-noise ( $L = 25$ ,  $\eta = 0.01$ ) lead to formation of groups that move in random directions. (c) High-density and large-noise (same as parameters in (a):  $L = 7$ ,  $\eta = 2.0$ ), but after some time and (d) High-density and low-noise ( $L = 5$ ,  $\eta = 0.1$ ) results in highly ordered motion.

$\theta_i(t + \delta t)$  have been calculated, each individual moves in that direction with speed  $s$  for a small time interval  $\delta t$ , after which all angles are re-computed.

The Vicsek model is therefore a simple model of SPPs in continuous space, where each individual updates their direction of motion synchronously at discrete time steps based on Eq. (1). Nevertheless, the model exhibits a surprisingly rich variety of spatial patterns of collective movement. For example, it is evident from Fig. 1 that ordering is facilitated by both low levels of noise and high densities of individuals. By calculating the average alignment of the individuals' motion, Vicsek defined a global 'order parameter' in analogy with the polarization of a ferromagnet. Mathematically, this is given by the scalar quantity

$$m(t) = \frac{1}{N s} \left| \sum_{i=1}^N \mathbf{v}_i(t) \right|, \quad (2)$$

where  $\mathbf{v}_i$  represents the velocity vector of individual  $i$  at time  $t$ . The normalisation includes  $s$ , which is the speed of each individual. The quantity  $m$  is popularly known as the Vicsek order-parameter in the physics literature; when close to 0 the group exhibits disordered motion, whilst when close to 1

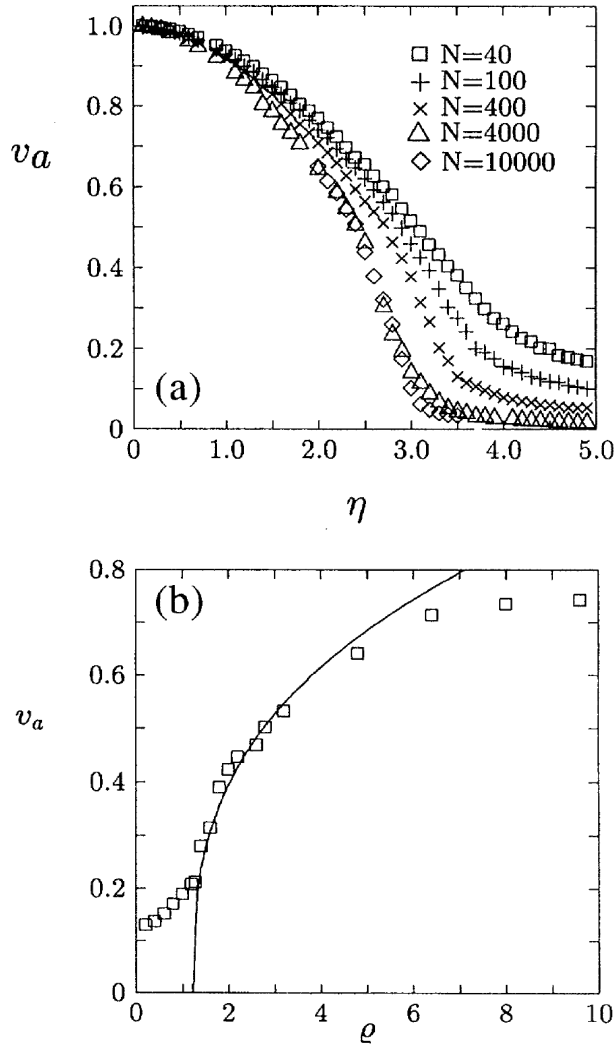


Figure 2: Phase diagram of the Vicsek model, reproduced here with permission from *American Physical Society: Physical Review Letters* (Vicsek et al., 1995). The order parameter (denoted as  $v_a$  in the Figure above; we adopt the notation  $m$  in this manuscript for the equivalent quantity) which captures the degree of alignment or polarisation of the entire population of particles. It shows features of phase-transition from order to disorder as the strength of noise ( $\eta$ ) increases in (a) and as the density of particles ( $\rho$ ) increases in (b). See Vicsek et al. (1995) for parameter values and other details.

the group is highly polarised, *i.e.*, all individuals move in the same direction. Notably, Vicsek et al. (1995) showed via numerical simulations that the ensemble average of this quantity exhibits a phase transition in two-dimensions as a function of increasing density, and decreasing noise (Fig. 2).

Since Vicsek's original paper, an array of similar SPP models of collective motion have been developed in continuous and discrete one-, two- and three-dimensional space (Mogilner and Edelstein-Keshet, 1999; Czirók et al., 1999b; Inada and Kawachi, 2002; Chowdhury et al., 2002; Couzin et al., 2002; Grégoire and Chaté, 2004; Nishinari et al., 2006; Chaté et al., 2008; Strömbom, 2011). Several

of these studies rely on numerical simulations to elucidate how simple microscopic interactions result in large scale collective motion. A number of analytical theories have been developed to describe the behaviour of the order-parameter  $m$  in Vicsek-like and other collective motion models (Toner and Tu, 1995; Czirók et al., 1999a; Jadbabaie et al., 2003; Ginelli, 2016). However, much of their focus is on understanding behaviour at the macroscopic scale *i.e.*, in the limit of infinite population/group sizes, ignoring the role of stochastic effects arising from finite population/group sizes (Kunwar et al., 2004; Aldana et al., 2007; Baglietto and Albano, 2009; Ramaswamy, 2010; Romanczuk and Schimansky-Geier, 2012; Marchetti et al., 2013).

Here, our aim is to demonstrate a ‘first principles’ approach to the derivation of *mesoscopic* models for the order parameter  $m$ , where noise is a function of both individual behaviours (which are stochastic) and finite size of groups. This is in contrast to the many *ad-hoc* methods of including stochastic effects, such as simply appending a noise term to otherwise mean-field dynamics, for example. For analytical tractability, we will demonstrate the construction of such mesoscopic descriptions from microscopic rules that are simpler than the Vicsek model. Our aim is that this chapter be accessible to readers at the graduate, or even advanced undergraduate, level in numerate subjects like mathematics, physics, statistics and quantitative biology. Although we endeavour to explain most concepts and techniques as they are introduced (occasionally referring to standard books for certain technical/detailed steps), basic familiarity of the reader with the following subjects will be helpful: dynamical-system based analyses of ordinary differential equations (ODEs) (Strogatz, 2018), probability theory, stochastic differential equations (SDEs), Ito-calculus, Master equations and Fokker-Planck equations (Gardiner, 2009).

Before proceeding further, we state our goals in more specific terms. Given a microscopic model of interactions between individuals, we would like to derive an SDE for a coarse variable that quantifies some aspect of the collective. If the coarse-variable is  $m$ , at mesoscopic scales where stochasticity is important, we expect the dynamical equation to be of the form

$$\frac{dm}{dt} = f(m) + g(m)\eta(t), \quad (3)$$

where  $\eta(t)$  is so-called delta-correlated Gaussian white noise with zero mean— *i.e.*,  $\langle \eta(t) \rangle = 0$  and  $\langle \eta(t)\eta(t') \rangle = \delta(t - t')$  [see Gardiner (2009) for more details]. This is an example of an SDE, and is sometimes also referred to as a Langevin equation. The function  $f(m)$  is referred to as the *deterministic* or *drift* term, whilst  $g(m)$  is often called the *stochastic* or *diffusion* term (Kolpas et al., 2007; Yates et al., 2009; Kolpas, 2008). If  $g(m)$  is constant, the strength of noise is independent of the state of the system, and noise can be thought of as external, or *additive*, to the deterministic dynamics. On the other hand, if  $g(m)$  is not constant, the strength of the noise depends on the current state  $m(t)$ . Such noise is called multiplicative, or state-dependent, and is known to produce unexpected results (Horsthemke, 1984; Altschuler et al., 2008; Lawson et al., 2013; Boettiger, 2018). In the following sections, we will not only describe how to derive equations of the form (3) from given probabilistic rules for individual-level behaviour, but also provide some heuristic insight into the different types of behaviours that can arise.

### 3. Mesoscopic description of a pairwise binary-choice model

In this section, we illustrate two complementary methods for deriving mesoscopic dynamical descriptions of collective behaviour from first principles. To do so, we choose a simple microscopic model of binary-choice, used to describe foraging animals that must choose between two food sources (Kirman, 1993; Biancalani et al., 2014), but also applied in several other diverse contexts, such as traders in financial markets (Kirman, 1993; Alfarano et al., 2008), and the recruitment

of cell signaling molecules (Altschuler et al., 2008). Here, individuals can collect food from one of two sources, labeled by  $i = 1, 2$ , which can be thought of as being located at either end of a long line. The food source to which each individual is moving therefore determines its direction, either positive or negative, which is denoted by  $X_i$ . The proportion of the colony (total number of individuals,  $N$ ) moving in a given direction is written using lowercase  $x_i = N_i/N$ , where  $N_i$  is simply the number of individuals with direction of motion  $X_i$ .

### 3.1. The model

As with any model of collective decision making, the choice that any individual makes is influenced by its *interactions* with the group (*i.e.*, what others are doing) as well as external factors. In this section, we focus first on pairwise interactions, with higher-order interactions (specifically, ternary interactions) described in Section 4. For the case of our pairwise binary-choice model, we imagine a continuous-time stochastic protocol whereby individuals can interact in two different ways.

Firstly, individuals can *copy* each other. For example, an interaction between a focal individual moving towards source 1 with another moving towards source 2 causes the focal individual to copy the other, and therefore switch to move towards the other source, 2. Likewise, an interaction between a focal individual of direction  $X_2$  with another of direction  $X_1$  causes the focal individual to switch to move towards source 1. These interactions can be represented in the same way as chemical reactions, writing:



and



Such copying interactions, occurring at a specific rate  $c$ , lead to an auto-catalytic process wherein an individual's chance of switching directions depends on the proportion of individuals already moving in that direction.

Secondly, the model also incorporates a level of *random* choice, where individuals ignore the actions of the others, and switch from their current food source spontaneously at a rate  $s$ . The corresponding 'chemical' reactions are:



and



Since the proportions of individuals going towards either source sum to unity, *i.e.*,  $x_1 + x_2 = 1$ , we can define a *coarse-variable*  $m = x_1 - x_2 = 1 - 2x_1$ , which takes values from  $-1$  to  $1$  and encapsulates the propensity of the group to be moving to either of the food sources. The extreme values of  $m$  correspond to consensus decision making, *i.e.*, all individuals collectively forage from source 1 ( $m = 1$ ) or source 2 ( $m = -1$ ). The values of  $m$  close to zero imply a lack of consensus, or collective behaviour, with equal proportions going towards either of the food sources. In-line with the previous section, we refer to  $m$  as the order parameter.

Indeed, let us compare the pairwise interaction binary-choice model (sometimes referred to as the 'ant model' in the literature) with the Vicsek model. The pairwise interaction model is a highly simplified representation of collective behaviour, analogous to both the classical Voter model (Cox and Griffeth, 1986) and the stepping stone model of population genetics (Kimura and Weiss, 1964). Unlike the Vicsek model, the rules are described via probabilistic reactions, rather than a difference equation. Further, here we ignore space, and assume that any individual can interact with any other individual in the population. Additionally, the update protocol is asynchronous *i.e.*,

individuals do not update their orientations simultaneously; this is in contrast to the synchronous update of orientations and positions of all individuals in the Vicsek model. Further, whilst the Vicsek model considers a continuous  $\theta$  (the angle/direction of movement), this model assumes only two sources of food, and hence two directions. (For completeness, we present an extension to the pairwise interaction model in Appendix B, where we permit four choices, in order to model movement in a two-dimensional space). We also note that the order parameter of the Vicsek model ranges from 0 (disorder) to 1 (order), whereas here, it ranges from  $-1$  to  $1$ , with both extremes representing order (consensus) and the value  $m = 0$  representing disorder (or lack of consensus).

Taken together, the aforementioned simplifications make the task of formally constructing mesoscopic equations relatively straightforward, whereas coarse-grained descriptions of the Vicsek model typically rely on symmetry arguments (Toner and Tu, 1995; Ramaswamy, 2010) and are harder to explicitly derive from the underlying microscopic model.

### 3.2. Constructing mesoscopic SDEs

We describe two complementary approaches to constructing a mesoscopic dynamical equation for the coarse-grained variable  $m$ , of the form (3). The first method is based on van Kampen’s system-size expansion method (Van Kampen, 1992), and is well known in the statistical physics community. Amongst other groups, the technique has been adopted extensively by McKane and colleagues for use in a variety of biological, ecological and epidemiological contexts (McKane and Newman, 2004, 2005; Biancalani et al., 2014). The second approach is called the chemical Langevin equations (CLEs), developed by Gillespie (2000). The latter method is prevalent in chemistry (Sotiropoulos and Kaznessis, 2011) and to some extent in the biological literature concerning gene regulatory networks (Simpson et al., 2009; El-Samad et al., 2006), biochemical pathway analysis (Rüdiger, 2014) and epidemiology (Colizza et al., 2007; Yuan and Allen, 2011; Wang et al., 2016). However, aside from a couple of studies (Datta et al., 2010; Joshi and Guttal, 2018) it is, to our knowledge, rarely used in the ecology literature.

#### 3.2.1. van Kampen’s system-size expansion of transition rates

We begin by summarising the step-by-step approach of this method: given a microscopic model, or protocol, the first step is to write how individual/microscopic rules translate into *transition rates* between different states of the system [denoted by the shorthand  $\mathbf{x} = \{x_1, x_2\}^T$ ]. The transition rates depend on the current state of the system and the system size (in this case, the number of individuals,  $N$ ). In the second step, using these transition rates, we write a *master equation* for the temporal evolution of the probability density function (PDF) for the system’s state,  $P(\mathbf{x}, t)$ . In the third step, we write the transition rates in terms of operators and Taylor-expand them for large but finite  $N$ , retaining only the two leading order terms. This provides a so-called *Fokker-Planck* equation for  $P(\mathbf{x}, t)$ , which approximates the aforementioned master equation. Then, we transform the state variables  $\mathbf{x}$  to the coarse-variable of interest (in this case,  $m$ ). Finally, we construct the SDE, or Langevin equation, that corresponds to the transformed Fokker-Planck equation.

*Transition rates:* For the model under consideration, since the individuals are indistinguishable, the state of the system is given by the variables  $x_1$  and  $x_2$ : the proportion of individuals moving in the negative and positive directions, respectively. Both  $x_1$  and  $x_2$  take discrete values in the range  $\{0, 1/N, \dots, N - 1/N, 1\}$ . Given an initial state  $(x_1, x_2)$ , a single reaction of the type (4a) results in the state  $(x_1 - 1/N, x_2 + 1/N)$ , whilst (4b) results in  $(x_1 + 1/N, x_2 - 1/N)$ . Both transitions occur at a rate  $c x_1 x_2$ , *i.e.*, the probability of picking two random individuals moving in different directions, multiplied by the rate at which they copy each other. Similarly, a single reaction of type (5a) also results in the state  $(x_1 - 1/N, x_2 + 1/N)$ , whilst (5b) results in  $(x_1 + 1/N, x_2 - 1/N)$ . Here the transitions occur at a rate  $s x_1$  and  $s x_2$ , respectively, which is just the probability of picking a given individual, multiplied by the rate at which they switch direction. Combining the above, we

write down the overall rate associated with a transition from state  $(x_1, x_2)$  to  $(x_1 - 1/N, x_2 + 1/N)$ , which is just

$$T_{21} = T\left(x_1 - \frac{1}{N}, x_2 + \frac{1}{N} \mid x_1, x_2\right) = c x_1 x_2 + s x_1. \quad (6)$$

Similarly, for the transition  $(x_1, x_2)$  to  $(x_1 + 1/N, x_2 - 1/N)$ , we have

$$T_{12} = T\left(x_1 + \frac{1}{N}, x_2 - \frac{1}{N} \mid x_1, x_2\right) = c x_2 x_1 + s x_2. \quad (7)$$

Here, the shorthand notation  $T_{ij} = T(x_i + 1/N, x_j - 1/N \mid x_i, x_j)$  has been introduced for convenience in the coming manipulations. We also note that, due to the constraint  $x_1 + x_2 = 1$ , technically only one of  $x_1$  or  $x_2$  is required to fully determine the state of the system, a point to which we will return later.

*Master equation:* We describe the evolution, or rate of change, of  $P(\mathbf{x}, t)$  by the influx of density associated with the state  $\mathbf{x}$  from that of the other states  $\mathbf{x}' \neq \mathbf{x}$ , minus the outflow of density from state  $\mathbf{x}$  to the other states  $\mathbf{x}' \neq \mathbf{x}$ . The resulting partial differential equation is called a master equation and is given by

$$\frac{\partial P(\mathbf{x}, t)}{\partial t} = \sum_{\mathbf{x}' \neq \mathbf{x}} [T(\mathbf{x} \mid \mathbf{x}') P(\mathbf{x}', t) - T(\mathbf{x}' \mid \mathbf{x}) P(\mathbf{x}, t)] \quad (8)$$

$$= \sum_{x'_1 \neq x_1} \sum_{x'_2 \neq x_2} [T(x_1, x_2 \mid x'_1, x'_2) P(x'_1, x'_2, t) - T(x'_1, x'_2 \mid x_1, x_2) P(x_1, x_2, t)] \quad (9)$$

$$= \sum_{x'_1 \neq x_1} \sum_{x'_2 \neq x_2} [T(x_1, x_2 \mid x'_1, x'_2) P(x'_1, x'_2, t)] - (T_{12} + T_{21}) P(x_1, x_2, t). \quad (10)$$

*Step operators:* The next step is to rewrite the master equation in terms of step-operators,  $\mathcal{E}_i^\pm$ , which are defined as

$$\mathcal{E}_i^\pm f(x_i) = f(x_i \pm \frac{1}{N}). \quad (11)$$

The key idea is to use such step operators to compactly replace the sum that appears in Eq. (10). For example, the first term of Eq. (10) can be drastically simplified by using both the aforementioned step operators and the previously introduced shorthand for transition rates:

$$\begin{aligned} \sum_{x'_1 \neq x_1} \sum_{x'_2 \neq x_2} T(x_1, x_2 \mid x'_1, x'_2) P(x'_1, x'_2, t) &= T\left(x_1, x_2 \mid x_1 - \frac{1}{N}, x_2 + \frac{1}{N}\right) P\left(x_1 - \frac{1}{N}, x_2 + \frac{1}{N}, t\right) \\ &\quad + T\left(x_1, x_2 \mid x_1 + \frac{1}{N}, x_2 - \frac{1}{N}\right) P\left(x_1 + \frac{1}{N}, x_2 - \frac{1}{N}, t\right) \\ &= \mathcal{E}_1^- \mathcal{E}_2^+ T_{12}(x_1, x_2) P(x_1, x_2, t) \\ &\quad + \mathcal{E}_1^+ \mathcal{E}_2^- T_{21}(x_1, x_2) P(x_1, x_2, t). \end{aligned} \quad (12)$$

Note that the operators act on all functions, and all arguments therein, that appear to its right hand side. The full master equation, now in the form of operators, is given by

$$\frac{\partial P(x_1, x_2, t)}{\partial t} = (\mathcal{E}_1^- \mathcal{E}_2^+ - 1) T_{12} P(x_1, x_2, t) + (\mathcal{E}_1^+ \mathcal{E}_2^- - 1) T_{21} P(x_1, x_2, t), \quad (13)$$

where the functional dependence of the rates  $T_{12}$  and  $T_{21}$  on the state  $(x_1, x_2)$  have been dropped for brevity.



*Taylor expansion:* We now recognise that for large  $N$  the action of the step operators may be approximated by a Taylor series. In doing so, we implicitly consider a continuous approximation of the variables  $x_i$ . Retaining only the first two terms in the expansion, we use the generic form

$$\mathcal{E}_i^\pm f(x_i) = f\left(x_i \pm \frac{1}{N}\right) = \left[1 \pm \frac{1}{N} \frac{\partial}{\partial x_i} + \frac{1}{2N^2} \frac{\partial^2}{\partial x_i^2}\right] f(x_i). \quad (14)$$

Applying this expansion scheme to Eq. (13) and simplifying, we get

$$\begin{aligned} \frac{\partial P(x_1, x_2, t)}{\partial t} &= \frac{1}{N} \left( \frac{\partial}{\partial x_2} - \frac{\partial}{\partial x_1} \right) [T_{12} P(x_1, x_2, t)] + \left( \frac{\partial}{\partial x_1} - \frac{\partial}{\partial x_2} \right) [T_{21} P(x_1, x_2, t)] + \\ &\quad \frac{1}{2N^2} \left( \frac{\partial}{\partial x_1} - \frac{\partial}{\partial x_2} \right)^2 [(T_{12} + T_{21}) P(x_1, x_2, t)]. \end{aligned} \quad (15)$$

Rearranging various terms, rescaling time according to  $t' = t/N$  and then dropping the prime for ease of notation, we get the canonical form of a Fokker-Planck equation

$$\frac{\partial P(x_1, x_2, t)}{\partial t} = \left[ - \sum_{i=1}^2 \frac{\partial [\mathcal{A}_i P(x_1, x_2, t)]}{\partial x_i} + \frac{1}{2N} \sum_{i,j=1}^2 \frac{\partial^2 [\mathcal{B}_{ij} P(x_1, x_2, t)]}{\partial x_i \partial x_j} \right], \quad (16)$$

where  $\mathcal{A}$  is vector and  $\mathcal{B}$  is a matrix whose elements are given, respectively, by

$$\mathcal{A}_i = T_{ij} - T_{ji}, \text{ and } \mathcal{B}_{ij} = (T_{ij} + T_{ji})(-1)^{i+j}. \quad (17)$$

Notice that our derivation of the Fokker-Planck equation (16) and the associated terms in Eqs. (17) make little reference to the pairwise interaction model. In other words, the above equations describing the time evolution of the PDF are based on very general features, and largely independent of the specific model under consideration. As a result, we may first apply this to the pairwise binary-choice model, before returning to re-use the same expression in Section 4 for the extension to ternary interactions. For the pairwise model, substituting Eqs. (6) and (7) into Eqs. (17), we get

$$\mathcal{A}_1 = s(x_2 - x_1) = -\mathcal{A}_2, \text{ and } \mathcal{B}_{ij} = [2cx_1x_2 + s(x_1 + x_2)](-1)^{i+j}. \quad (18)$$

*Mesoscopic SDE:* Given a Fokker-Planck equation for a PDF, it is, in principle, always possible to construct a system of corresponding SDEs in order to describe the stochastic variables whose statistics are described by that PDF. For details, we refer the reader to the classic book on stochastic processes by Gardiner (2009). For the pairwise interaction model, the system of SDEs that are equivalent to a Fokker-Planck equation with the terms (18), are:

$$\frac{dx_1}{dt} = \mathcal{A}_1 + \frac{1}{\sqrt{N}} \xi_1(t), \text{ and } \frac{dx_2}{dt} = \mathcal{A}_2 + \frac{1}{\sqrt{N}} \xi_2(t), \text{ where } \langle \xi_i(t) \xi_j(t') \rangle = \mathcal{B}_{ij} \delta(t - t'). \quad (19)$$

In the above SDEs,  $\xi_1$  and  $\xi_2$  represent noise sources that are correlated. Moreover,  $x_1$  and  $x_2$  are constrained by the fact that  $x_1 + x_2 = 1$ , and it is therefore possible to eliminate one of the two variables. To obtain a simpler SDE, which is still consistent with a Fokker-Planck description involving the coefficients (18), we therefore invoke the transformation  $\xi_i = \sum_{j=1}^2 \mathcal{G}_{ij} \eta_j$ , where  $\mathcal{B} = \mathcal{G}\mathcal{G}^T$  and the  $\eta_j$  ( $j = 1, 2$ ) each correspond to independent delta-correlated Gaussian white noises. Because  $\mathcal{B}$  and  $\mathcal{G}$  are square  $2 \times 2$  matrices, it is easy to see that  $\mathcal{G}_{ij} = (-1)^{i+j+1} \sqrt{2cx_1x_2 + s(x_1 + x_2)} / \sqrt{2}$ . Substituting this into Eqs. (19) we obtain,

$$\frac{dx_1}{dt} = s(x_2 - x_1) + \sqrt{\frac{2cx_1x_2 + s(x_1 + x_2)}{2N}} [\eta_2(t) - \eta_1(t)] = -\frac{dx_2}{dt}. \quad (20)$$

Introducing  $m = x_1 - x_2$  then yields

$$\frac{dm}{dt} = -2sm + \frac{1}{\sqrt{N}} \sqrt{c(1-m^2) + 2s} [\eta_2(t) - \eta_1(t)]. \quad (21)$$

We use the fact that the difference between two variables, each drawn from independent but identical Gaussian distributions, is statistically equivalent to simply drawing from a single Gaussian distribution. Therefore, the above SDE simplifies to

$$\frac{dm}{dt} = -2sm + \sqrt{\frac{2}{N}} \sqrt{c(1-m^2) + 2s} \eta(t). \quad (22)$$

Finally, it is helpful to move to a rescaled time  $t' = 2st$ . However, since the variance of the noise term depends on the timescale, care must be taken. Without wanting to digress too far on the subject of SDEs, the easiest course of action is to rescale the Fokker-Planck equation corresponding to (22) by multiplying it with  $dt/dt' = 1/2s$ . Relabeling  $t'$  as  $t$  and writing-down a new SDE, we get

$$\frac{dm}{dt} = -m + \sqrt{\frac{N_c}{N}} \sqrt{1-m^2 + 2s} \eta(t), \quad (23)$$

where  $s/c = s$  and  $N_c = 1/s$  (Biancalani et al., 2014). As before,  $\eta(t)$  is delta-correlated Gaussian white noise, *i.e.*,  $\langle \eta(t) \rangle = 0$  and  $\langle \eta(t) \eta(t') \rangle = \delta(t - t')$ .

In the Section 3.3, we continue the analyses of Eq. (23) by solving for the steady-state solution of the corresponding Fokker-Planck equation and by generating sample stochastic trajectories numerically. Before doing so, however, we demonstrate an alternative, and often complementary approach to the derivation of mesoscopic SDEs, known as the chemical Langevin equation approach (Gillespie, 2000).

### 3.2.2. Gillespie’s chemical Langevin approach

An alternative method for the construction of mesoscopic equations was developed by Gillespie (2000) in the context of many interacting chemical species, which provides a neat heuristic to write down SDEs directly from a set of chemical reactions. Here, as with van Kampen’s approach, the method accounts for the stochasticity that arises from finite population sizes. The mathematical arguments for the approach are described in detail by Gillespie (2000), where both the similarities and differences to van Kampen’s method are discussed at length. For completeness, we tersely recapitulate some of the arguments/steps in Appendix A. Given certain assumptions are satisfied, the procedure involves constructing so called *propensity functions* and *state change vectors/matrices*, and then simply assembling the SDE accordingly. We demonstrate this approach in the context of the pairwise interaction model described in Section 3.1.

*Propensity functions:* The propensity function, denoted by  $a_j(\mathbf{x})$ , represents the probability per unit time of reaction  $j$ . Here, as before,  $\mathbf{x} = \{x_1, x_2\}^\top$ , which represents the state of the system in terms of the concentration/proportion of individuals of different species. [Note that in Appendix A we follow Gillespie (2000) and define the propensity function in terms of the absolute number of individuals ( $N_i$ ) of each species present in the system, rather than concentrations, which are used here for comparison with van Kampen’s approach]. The reaction propensities are computed based on the principle of mass action, *i.e.*, that the probability of a reaction occurring at a given instant is equal to a specific rate multiplied by the product of the concentrations of all the constituent chemicals of that reaction at that time. Let us recall that the pairwise interaction model is described by the four microscopic rules or ‘chemical reactions’ set out in Eqs. (4a–5b). Consider the first reaction, which represents an individual originally moving towards source 1, who

copies the behaviour of another individual and changes to move towards source 2. The corresponding propensity function is just the copying rate  $c$  multiplied by the product of the proportion of individuals moving in direction 1 ( $x_1$ ) and the proportion of individuals moving in direction 2 ( $x_2$ ); thus,  $a_1(\mathbf{x}) = c x_1 x_2$ . Applying this procedure to the remaining reactions [(4b), (5a) and (5b)] yields the following propensity functions:

$$\begin{aligned} a_2(\mathbf{x}) &= c x_1 x_2, \\ a_3(\mathbf{x}) &= s x_1, \\ a_4(\mathbf{x}) &= s x_2. \end{aligned}$$

*State change matrix:* We then construct the state change, or stoichiometry, matrix  $\boldsymbol{\nu}$ , of which an element  $\nu_{ji}$  represents the change in the number of individuals of species  $i$  when the reaction  $j$  occurs. The rows of  $\boldsymbol{\nu}$  therefore correspond to the reactions and the columns represent the different species of the individuals. For the pairwise interaction model, for example, the first element in the second row represents a loss of one individual moving towards food source 1, and hence  $\nu_{21} = -1$ . Conversely, the second element in the second row represents a gain of an individual moving towards source 2, and hence  $\nu_{22} = 1$ . Accounting for all four reactions,  $\boldsymbol{\nu}$  is a  $4 \times 2$  matrix, given by

$$\boldsymbol{\nu} = \begin{bmatrix} -1 & 1 \\ 1 & -1 \\ -1 & 1 \\ 1 & -1 \end{bmatrix}. \quad (24)$$

*Chemical Langevin equations:* Using the propensity functions and the state change matrix, we can follow Gillespie's recipe and write-down the chemical Langevin equation(s). While we refer the reader to the mathematical arguments in (Gillespie, 2000) and Appendix A, the basic idea is as follows. Each reaction  $j$  causes a change in the concentration of species  $i$  per unit time, which is given by the product of rate of that reaction [*i.e.*, the propensity function  $a_j(\mathbf{x})$ ] with the associated change in that species numbers (*i.e.*, the stoichiometry matrix entry  $\nu_{ji}$ ). Thus, the expected rate of change in the concentration of species  $i$  due to reaction  $j$  will be  $\nu_{ji} a_j(\mathbf{x})$ . However, chemical reactions are stochastic events and the above term yields only an expected number of reactions per unit time. To take account of stochastic fluctuations, Gillespie uses the fact that, for large enough  $N$ , the change in the concentration of species  $i$  due to reaction  $j$  can be approximated by a normally distributed random variable for which the variance and the mean are both equal to the the propensity of the reaction  $j$ . Applying this principle to all reactions  $j$  that result in a change in concentration of chemical  $i$ , we obtain the system of 'chemical' Langevin equations

$$\frac{dx_i(t)}{dt} = \sum_{j=1}^r \nu_{ji} a_j(\mathbf{x}) + \frac{1}{\sqrt{N}} \sum_{j=1}^r \nu_{ji} [a_j(\mathbf{x}(t))]^{1/2} \eta_j(t), \text{ for } i = 1, \dots, n. \quad (25)$$

where  $n$  is the total number of species/chemicals,  $r$  is the total number of reactions,  $N$  is the total number of individuals in the entire system, and  $\eta_j$  are the usual delta-correlated Gaussian noise sources with zero mean and unit variance.

Applying this scheme to the pairwise interaction model, we set  $i = 1$ , which represents the proportion of ants moving in the direction of food source 1. The first, so-called *deterministic*, term of the Langevin equation for  $dx_1/dt$ , is found to be

$$\begin{aligned} \sum_{j=1}^r \nu_{j1} a_j(\mathbf{x}) &= \nu_{11} a_1 + \nu_{21} a_2 + \nu_{31} a_3 + \nu_{41} a_4, \\ &= -c x_1 x_2 + c x_1 x_2 - s x_1 + s x_2, \\ &= s(x_2 - x_1). \end{aligned}$$

Likewise, the second, *stochastic*, term can be computed as

$$\sum_{j=1}^r \nu_{j1} [a_j(\mathbf{x})]^{1/2} \eta_j(t) = \nu_{11} \sqrt{a_1} \eta_1(t) + \nu_{21} \sqrt{a_2} \eta_2(t) + \nu_{31} \sqrt{a_3} \eta_3(t) + \nu_{41} \sqrt{a_4} \eta_4(t), \quad (26)$$

$$= -\sqrt{c x_1 x_2} \eta_1(t) + \sqrt{c x_1 x_2} \eta_2(t) - \sqrt{s x_1} \eta_3(t) + \sqrt{s x_2} \eta_4(t). \quad (27)$$

Putting these two expressions together, the CLE for the dynamics of the variable  $x_1$  is given by

$$\frac{dx_1}{dt} = s(x_2 - x_1) + \frac{1}{\sqrt{N}} \left[ -\sqrt{c x_1 x_2} \eta_1(t) + \sqrt{c x_1 x_2} \eta_2(t) - \sqrt{s x_1} \eta_3(t) + \sqrt{s x_2} \eta_4(t) \right]. \quad (28)$$

It is easy to see that the analogous expression for  $x_2$  satisfies  $dx_2/dt = -dx_1/dt$ , which is consistent with the constraint  $x_1 + x_2 = 1$ . To obtain the equation for the order parameter  $m$ , we note that  $m = x_1 - x_2$  and find

$$\frac{dm}{dt} = -2sm + \frac{2}{\sqrt{N}} \left[ \sqrt{\frac{c(1-m^2)}{4}} (\eta_2(t) - \eta_1(t)) - \sqrt{s \frac{1+m}{2}} \eta_3(t) + \sqrt{s \frac{1-m}{2}} \eta_4(t) \right]. \quad (29)$$

By substituting  $c = 1$ , rescaling time  $t' \rightarrow 2st$  and writing  $t' = t$ , we get

$$\frac{dm}{dt} = -m + \sqrt{\frac{N_c}{N}} \left[ \sqrt{1-m^2} \eta'_1(t) - \sqrt{s(1+m)} \eta'_2(t) + \sqrt{s(1-m)} \eta'_3(t) \right]. \quad (30)$$

Since the noise sources are Gaussian and independent, the term in the square brackets is equivalent to a single noise source with a variance equal to the  $\ell^2$ -norm of the variances of the individual noise sources,  $\eta'_1$ ,  $\eta'_2$  and  $\eta'_3$ . The result is that

$$\frac{dm}{dt} = -m + \sqrt{\frac{N_c}{N}} \sqrt{1-m^2 + 2s} \eta(t), \quad (31)$$

where  $N_c = 1/s$ . This is the same stochastic differential equation that we derived using the system-size expansion approach (23), thus both approximations/methods yield the same mesoscopic description in this case. In the Discussion section, we comment on how the two methods are related, and how they do not necessarily yield the same equations for the extended version of a pairwise interaction model in two spatial dimensions—*i.e.*, with more than two choices—as set out in Appendix B.

### 3.3. Characterising mesoscopic dynamics

In this section, we employ three different methods to characterise the previously obtained mesoscopic SDE describing the dynamical behavior of the order parameter,  $m$  [Eqs. (23) or (31)]. Before doing so, we make some remarks on the qualitative features of the equation.

First, in the macroscopic ( $N \rightarrow \infty$ ) limit, the system exhibits deterministic dynamics given by  $dm/dt = -m$ . This implies that order decays exponentially with time, reaching the *deterministic stable state*  $m^* = 0$  asymptotically. In this state, an equal number of individuals choose food sources 1 and 2. Hence, the macroscopic system is disordered with no consensus or alignment among individuals.

Second, in the mesoscopic description ( $N$  large but finite) both the deterministic and stochastic terms of Eq. (23) are required to govern the dynamics of  $m$ . Here, the noise prefactor depends on the current state,  $m$ ; such a feature is called multiplicative or state-dependent noise. In this case, the noise strength is maximum when the system is disordered (*i.e.*,  $m = 0$ ) and minimum

when system is ordered (*i.e.*,  $m = \pm 1$ ). Furthermore, the strength of this noise becomes larger for decreasing system sizes.

As we show below, the interplay between a deterministic term that pulls the system towards disorder and a stochastic term that does the opposite can produce interesting and often counter-intuitive dynamics.

### 3.3.1. Steady-state solution of the Fokker-Planck equation

SDEs describe how to realise trajectories of stochastic variable(s). Whilst often preferable for the purposes of gaining heuristic insight, or numerical implementation, they are equivalent to equations of the Fokker-Planck type, which are *partial* differential equations (PDEs) for the time-dependent probability distribution that governs the behaviour of such stochastic variable(s). For example, for an SDE of the form  $dm/dt = f(m) + g(m)\eta(t)$  (understood according to the Itô convention), the corresponding Fokker-Planck equation is given by (Gardiner, 2009)

$$\frac{\partial P(m, t)}{\partial t} = -\frac{\partial}{\partial m} [f(m)P(m, t)] + \frac{1}{2} \frac{\partial^2}{\partial m^2} [g^2(m)P(m, t)]. \quad (32)$$

In most cases, it is not possible to solve this equation analytically. However, it is often possible to solve this equation for the time-independent steady-state. We set  $\partial P(m, t)/\partial t = 0$  and denote the steady state PDF by  $P_s(m)$ , giving

$$\frac{\partial}{\partial m} [f(m)P_s(m)] = \frac{1}{2} \frac{\partial^2}{\partial m^2} [g^2(m)P_s(m)]. \quad (33)$$

Integrating both sides with respect to  $m$ , we get

$$f(m)P_s(m) = \frac{1}{2} \frac{\partial}{\partial m} [g^2(m)P_s(m)] + c_0, \quad (34)$$

where  $c_0$  is the integration constant. Under the assumption of no-flux boundary conditions,  $c_0 = 0$ . We integrate the above equation again and find that

$$P_s(m) = \frac{1}{P_0} \exp \left[ 2 \int_{m_0}^m \frac{f(m') - g(m')g'(m')}{g^2(m')} dm' \right], \quad (35)$$

where  $P_0$  is the normalization constant. Applying this to the mesoscopic description of the pairwise interaction model (23) where  $f(m) = -m$  and  $g(m) = \sqrt{N_c/N} \sqrt{1 + 2s - m^2}$ , we get

$$\frac{\partial P(m, t)}{\partial t} = \frac{\partial}{\partial m} [mP(m, t)] + \frac{N_c}{2N} \frac{\partial^2}{\partial m^2} [(1 + 2s - m^2)P(m, t)], \quad (36)$$

whose steady-state solution is given by (Biancalani et al., 2014)

$$P_s(m) = \frac{1}{\mathcal{P}_0} \frac{1}{(1 + 2s - m^2)^{1 - N/N_c}}, \quad (37)$$

where  $N_c = 1/s$  and  $\mathcal{P}_0$  is the normalisation constant. In Figure 3, we plot the steady-state distribution as a function of  $N$ .

### 3.3.2. Numerical integration of the mesoscopic SDE

Realisations of the stochastic trajectories of  $m(t)$ , governed by  $P(m, t)$ , can be obtained most easily by numerical integration of the SDE (23). There exist more complicated schemes, but here we choose an initial value  $m(t = 0) = m_0$  and employ a simple Euler-Murayama approach (Press et al., 1996), which corresponds to the difference equation

$$\Delta m = -m \Delta t + \sqrt{\frac{N_c}{N}} \sqrt{1 + 2s - m^2} \sqrt{\Delta t} \eta(t), \quad (38)$$

where  $\Delta t$  is a small fixed time interval. In the cases where  $P(m, t)$  cannot be obtained from the Fokker-Planck equation, we may repeat the above process a large number of times with different initial conditions and then plot the normalized histogram of  $m$ . The result converges, at long times, to the steady-state  $P_s(m)$ . In Figure 3, we display the time series and the PDF of  $m$  for different values of system size  $N$ .

### 3.3.3. Gillespie simulations of the microscopic model

In both the system-size expansion and the chemical Langevin approach, we assume finite but large systems for deriving Fokker-Planck and hence SDEs. To verify these approaches, we employ stochastic simulations (Gillespie, 1976, 1977) that are an exact representation of the master equation which describes the underlying microscopic process. Whilst Figure 3 presents results using the original scheme presented by Gillespie, there have since been many studies that improve both the speed and accuracy of the method. Interested readers are referred to studies such as Erban and Chapman (2009), which concerns improving the accuracy of the algorithm, and methods like  $\tau$ -leaping (Gillespie, 2001) for accelerating the speed of simulations.

### 3.4. Results for the pairwise interaction model

We now present the results from all three approaches in order to understand both the dynamics and steady-state properties of the order parameter for the pairwise interaction model.

The steady state solution of the Fokker-Planck equation predicts a group-size dependent PDF of the order parameter  $m$  (bottom row of Figure 3). Specifically, for large group sizes ( $N > N_c$ ) the PDF  $P_s(m)$  is unimodal with the mode occurring at  $m = 0$ . This implies that the most likely state is a disordered state consistent with the deterministic fixed point of the macroscopic/deterministic description. By contrast, for small group sizes  $N < N_c$ , the steady-state PDF  $P_s(m)$  is bimodal, with modes at  $m = \pm 1$ . Therefore, the system spends most of its time in highly ordered states. These two states correspond to a consensus decision that results in clear collective movement of individuals in a single direction.

The PDF obtained from repeated numerical integration of the SDE (23) produces qualitatively similar results as the analytical solution of the Fokker-Planck equation indicating minimal transient dynamics before reaching the steady state. The advantage of numerical simulation of the SDE is that we can also visualise the time series of the order parameter  $m$  (— in top panel, in Figure 3). We find that, for smaller group sizes,  $m$  frequently switches back and forth between two ordered states at  $m = 1$  and  $m = -1$ . However, this is clearly not the case with larger groups, which spend large amounts of time in a disordered  $m = 0$  state.

As expected, both the steady-state solution to the Fokker-Planck equation and repeated numerical integration of the SDE qualitatively match with the Gillespie simulations. Of course, as system size decreases, the results diverge slightly, which highlights the fact that the mesoscopic descriptions are only approximations of the underlying microscopic behaviour.

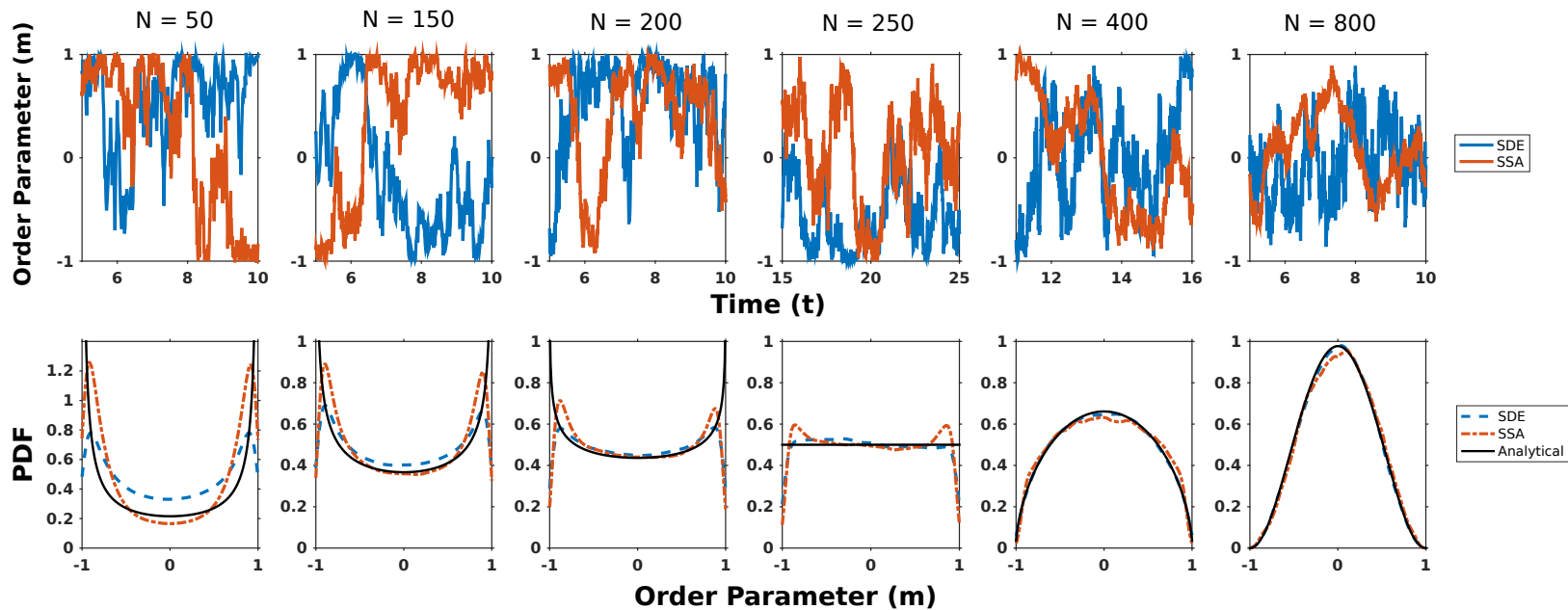


Figure 3: Dynamics and steady-state properties of the order-parameter or collective behaviour ( $m$ ) for the pairwise interaction model. Top row: Blue line (—) indicates numerical integration of the analytically derived SDE equation (23) whereas the orange line (—) shows Gillespie simulations of the model. Bottom row: Steady-state distribution of the order-parameter  $m$  obtained by numerical integration of SDE, Gillespie simulations and the analytical solutions of the Fokker-Planck equation for the model are shown by the black line (—).  $N_c = 250$

#### 4. Ternary interaction model for binary choice

We now present a simple extension of the pairwise interaction model that includes higher-order interactions. This model of collective behaviour was originally developed by Dyson et al. (2015) to explain the quantitative behaviour of a march of locusts in a one-dimensional arena (Buhl et al., 2006) and incorporates interactions between three individuals in addition to the previously discussed pairwise interactions; we refer to this model as the ‘ternary interaction model’. Once again, we apply both the system-size expansion and chemical Langevin approaches to derive a mesoscopic description.

As in the pairwise model, individuals move towards food source 1 or 2 depending on both their interactions with others and random factors. We once again assume that individuals spontaneously switch at a rate  $s$  between food sources/directions



Likewise, we also retain the copying interactions, occurring at a rate  $c$ , of the pairwise interaction model, given by



The new component of this model is a higher-order interaction, where three individuals interact. The reaction occurs at a specific rate  $h$ , and results in all individuals moving in the direction of the majority. Depending on whether  $X_1$  or  $X_2$  was in the majority at the time of interactions, one of the two following reactions occur:



We note that Schulze and Stauffer (2005) use a similar model to study evolution of language. In that model, a focal individual modifies its language spontaneously at a rate  $p$ , copies the language of a randomly chosen individual at a rate  $q$ , and finally, with a probability  $(1-x)^2r$ , the individual chooses the the language spoken by the fraction  $x$  of the population. This last reaction is identical to the ternary interaction set out in Eqs. (41).

##### 4.1. Constructing a mesoscopic SDE for the ternary interaction model

As we did before with the pairwise interaction model, we now apply both the system-size expansion and the chemical Langevin equation methods in order to derive a mesoscopic equation for the order parameter  $m = x_1 - x_2$ .



#### 4.1.1. van Kampen's system-size expansion of transition rates

*Transition Rates:* The state variables of the system are again  $x_1$  and  $x_2$ : the proportion of individuals moving in the direction of food sources 1 and 2, respectively. Similarly, since  $x_1 + x_2 = 1$ , one of either  $x_1$  or  $x_2$  can completely describe the state of the system. The transition rates  $T_{21}$  and  $T_{12}$  are the same as in the pairwise interaction model, except they must also incorporate reactions (41a) and (41b). The additional rates follow the ‘mass action’ rationale set out previously, giving

$$T_{21} = T \left( x_1 - \frac{1}{N}, x_2 + \frac{1}{N} \middle| x_1, x_2 \right) = s x_1 + c x_1 x_2 + h x_1 x_2^2, \quad (42)$$

and

$$T_{12} = T \left( x_1 + \frac{1}{N}, x_2 - \frac{1}{N} \middle| x_1, x_2 \right) = s x_2 + c x_1 x_2 + h x_1^2 x_2. \quad (43)$$

*Fokker-Planck equation:* Next, we substitute these transition rates into the general form of the Fokker-Planck equation for binary-choice models (15), where we note that the steps from Eq. (10) to Eq. (15) are independent of model interaction details. Therefore, we get

$$\frac{\partial P(x_1, x_2, t)}{\partial t} = \left[ - \sum_{i=1}^2 \frac{\partial [\mathcal{A}_i P(x_1, x_2, t)]}{\partial x_i} + \frac{1}{2N} \sum_{i,j=1}^2 \frac{\partial^2 [\mathcal{B}_{ij} P(x_1, x_2, t)]}{\partial x_i \partial x_j} \right], \quad (44)$$

where,

$$\mathcal{A}_1 = T_{12} - T_{21} = s(x_2 - x_1) + h x_1 x_2 (x_1 - x_2), \quad (45)$$

$$\mathcal{A}_2 = -\mathcal{A}_1, \quad (46)$$

$$\mathcal{B}_{ij} = (T_{ij} + T_{ji})(-1)^{i+j} = (-1)^{i+j} [s(x_1 + x_2) + 2c x_1 x_2 + h x_1 x_2 (x_1 + x_2)]. \quad (47)$$

*Mesoscopic SDE:* The coupled SDEs that correspond to realisations of the above Fokker-Planck equation are given by

$$\frac{dx_1}{dt} = \mathcal{A}_1 + \frac{1}{\sqrt{N}} \xi_1(t), \text{ and } \frac{dx_2}{dt} = \mathcal{A}_2 + \frac{1}{\sqrt{N}} \xi_2(t), \text{ where } \langle \xi_i(t) \xi_j(t') \rangle = \mathcal{B}_{ij} \delta(t - t'). \quad (48)$$

Using the same set of manipulations that we followed while analysing the pairwise interaction model, we obtain the mesoscopic equation for the order parameter  $m$  for the ternary interaction model. To do so, we use the transformation:  $\xi_i = \sum_{j=1}^2 \mathcal{G}_{ij} \eta_j$ , such that  $\mathcal{G}$  satisfies  $\mathcal{B} = \mathcal{G} \mathcal{G}^T$ . We find that

$$\mathcal{G}_{ij} = (-1)^{i+j+1} \sqrt{s(x_1 + x_2) + 2c x_1 x_2 + h x_1 x_2 (x_1 + x_2)} / \sqrt{2}.$$

After further transforming to  $m = x_1 - x_2$ , we obtain the mesoscopic dynamical equation (Dyson et al., 2015)

$$\frac{dm}{dt} = -2sm + \frac{h}{2} m(1 - m^2) + \frac{2}{\sqrt{N}} \sqrt{s + \frac{2c + h}{4} (1 - m^2)} \eta(t), \quad (49)$$

which, under the time rescaling  $t' = 2st$ , recovers the mesoscopic equation of the pairwise interaction model on setting  $h = 0$ .

#### 4.1.2. Chemical Langevin approach

As in Section 3.2.2, we define both propensity functions  $a_j(\mathbf{x})$  and the state change, or stoichiometry, vector  $\boldsymbol{\nu}$  for the ternary interaction model (Table 1). To derive the relevant ternary mesoscopic equation, we substitute both  $a_j(\mathbf{x})$  and  $\boldsymbol{\nu}$  from Table 1 into the chemical Langevin equations,

$$\frac{dx_i(t)}{dt} = \sum_{j=1}^r \nu_{ji} a_j(\mathbf{x}) + \frac{1}{\sqrt{N}} \sum_{j=1}^r \nu_{ji} [a_j(\mathbf{x})]^{1/2} \eta_j(t), \text{ for } i = 1, \dots, n, \quad (50)$$

where  $n$  is the number of species,  $r$  is the number of reactions,  $N$  is the total number of individuals, and  $\eta_j$  are Gaussian white noise sources with zero mean and correlation  $\langle \eta_i(t) \eta_j(t') \rangle = \delta_{ij} \delta(t - t')$ .

S. No. (j)	Reaction	Propensity	$\boldsymbol{\nu}_{j1}$	$\boldsymbol{\nu}_{j2}$
1	$X_1 \xrightarrow{s} X_2$	$sx_1$	-1	1
2	$X_2 \xrightarrow{s} X_1$	$sx_2$	1	-1
3	$X_1 + X_2 \xrightarrow{c} 2X_1$	$cx_1x_2$	1	-1
4	$X_1 + X_2 \xrightarrow{c} 2X_2$	$cx_1x_2$	-1	1
5	$2X_1 + X_2 \xrightarrow{h} 3X_1$	$hx_1^2x_2$	1	-1
6	$2X_2 + X_1 \xrightarrow{h} 3X_2$	$hx_1x_2^2$	-1	1

Table 1: Reactions in the higher order interaction model, their propensities and the state change vector

As an example, consider the variable  $x_1$ . The deterministic term of the CLE is given by

$$\begin{aligned} \sum_{j=1}^r \nu_{j1} a_j(\mathbf{x}) &= \nu_{11} a_1 + \nu_{21} a_2 + \nu_{31} a_3 + \nu_{41} a_4 + \nu_{51} a_5 + \nu_{61} a_6 \\ &= -sx_1 + sx_2 + cx_1x_2 - cx_1x_2 + hx_1^2x_2 - hx_1x_2^2 \\ &= s(x_2 - x_1) + hx_1x_2(x_1 - x_2). \end{aligned}$$

The stochastic term is given by

$$\begin{aligned} \sum_{j=1}^r \nu_{j1} [a_j(\mathbf{x})]^{1/2} &= \nu_{11} \sqrt{a_1} \eta_1(t) + \nu_{21} \sqrt{a_2} \eta_2(t) + \nu_{31} \sqrt{a_3} \eta_3(t) + \nu_{41} \sqrt{a_4} \eta_4(t) \\ &\quad + \nu_{51} \sqrt{a_5} \eta_5(t) + \nu_{61} \sqrt{a_6} \eta_6(t) \\ &= -\sqrt{sx_1} \eta_1 + \sqrt{sx_2} \eta_2 + \sqrt{cx_1x_2} \eta_3 - \sqrt{cx_1x_2} \eta_4 + \sqrt{hx_1^2x_2} \eta_5 - \sqrt{hx_1x_2^2} \eta_6. \end{aligned}$$

As before, it is easy to show that  $dx_1/dt = -dx_2/dt$ , because  $\nu_{j1} = -\nu_{j2}$ , for all  $j$ . As noise sources  $\eta_1$  to  $\eta_6$  are independent we may combine them into a single noise source to obtain

$$\sum_{j=1}^r \nu_{j1} [a_j(\mathbf{x})]^{1/2} = \sqrt{s(x_1 + x_2) + 2cx_1x_2 + hx_1x_2(x_1 + x_2)} \eta(t).$$

Hence, the CLE for the higher order interaction model in terms of variable  $x_1$  and  $x_2$  is given by

$$\frac{dx_1}{dt} = s(x_2 - x_1) + hx_1x_2(x_1 - x_2) + \frac{1}{\sqrt{N}} \sqrt{s(x_1 + x_2) + 2cx_1x_2 + hx_1x_2(x_1 + x_2)} \eta(t) = -\frac{dx_2}{dt}. \quad (51)$$

Substituting  $m = x_1 - x_2$  and using the constraint  $x_1 + x_2 = 1$ , we get

$$\frac{dm}{dt} = -2sm + \frac{h}{2}m(1 - m^2) + \frac{2}{\sqrt{N}}\sqrt{s + \frac{2c+h}{4}(1 - m^2)}\eta(t). \quad (52)$$

This mesoscopic dynamical equation in  $m$ , for the one dimensional ternary interaction model, derived using the chemical Langevin approach is exactly the same equation derived using the system-size expansion method. Therefore, we again see that both methods give exactly same results for one dimensional/uni-variate models.

#### 4.2. Characterising mesoscopic dynamics

We now turn to characterising the mesoscopic SDE (49) of the ternary interaction model both numerically and analytically. The methods are similar to the pairwise interaction model (Section 3.3).

##### 4.2.1. Steady-state solution of the Fokker-Planck equation

The deterministic and the stochastic terms of the mesoscopic equation for the ternary interaction model are  $f(m) = -2sm + hm(1 - m^2)/2$ , and  $g(m) = 2\sqrt{(s + (2c + h)(1 - m^2)/4)}/N$ , respectively. Therefore, the Fokker-Planck equation for the ternary interaction model is given by

$$\frac{\partial P(m, t)}{\partial t} = \frac{\partial}{\partial m} \left\{ \left[ 2sm - \frac{h}{2}m(1 - m^2) \right] P(m, t) \right\} + \frac{2}{N} \frac{\partial^2}{\partial m^2} \left\{ \left[ s + \frac{2c+h}{4}(1 - m^2) \right] P(m, t) \right\}. \quad (53)$$

Using the general expression for steady state PDF given by Eq. (35) (Gardiner, 2009), we get

$$P_s(m) = \frac{1}{P_0} [4s + (2c + h)(1 - m^2)]^{\frac{4Ns(c+h)}{(2c+h)^2} - 1} e^{-\frac{hm^2N}{2(2c+h)}}, \quad (54)$$

where  $P_0$  is the normalization constant (Dyson et al., 2015). In Figure 4, we plot this expression for different values of  $N$ .

##### 4.2.2. Numerical integration of the mesoscopic SDE

We applied the Euler-Murayama scheme to the SDE (49) in exactly the same way as Section 3.3.2. The time series and the probability density function thus obtained are shown in Figure 4 for different values of  $N$ .

##### 4.2.3. Gillespie simulations of the microscopic model

We implement the Gillespie algorithm in the same way as described in Section 3.3.3. We choose the sampling time as  $1/s$ , independent of system size. We later rescaled the time  $t = t'/N$  to match the timescale of the mesoscopic equation (49). The results of these simulations are presented in Figure 4.

#### 4.3. Results for the ternary interaction model

The steady-state solution of the Fokker-Planck equation is bimodal for all group sizes (— in bottom row, Fig. 4). The two modes of the distribution are however less distinct for small system sizes, becoming more prominent with increasing system size. Increasing the rate of higher-order interactions ( $h$ ) moves the location of the distribution modes to larger values of  $m$ . This implies that the system size only has quantitative but not qualitative influence on the steady state distribution of the order parameter. The effect is therefore in sharp contrast to the pairwise interaction model,

where increasing system size resulted in a transition from bimodal to unimodal distribution of  $m$ . Specifically, in the pairwise interaction model we observed two clear modes for small systems whereas, for the ternary interaction model, this corresponds to large system sizes.

To understand these results, consider the deterministic limit of the ternary interaction model's SDE. The  $N \rightarrow \infty$  limit of equation (49) has three fixed points  $(0, \pm\sqrt{(h-4s)/h})$ . For  $h > 4s$ , three real roots exist, of which  $m^* = \pm\sqrt{(h-4s)/h}$  are stable since  $f'(m^*) < 0$ . Visual inspection of two modes in the steady state PDF reveals that they are indeed near the location of these two deterministic stable fixed points of the dynamical equation for all values of the system size  $N$ . This is unlike the pairwise interaction model where the equation has only one stable fixed point at  $m = 0$ , but nevertheless has a bimodal PDF whose modes are away from  $m = 0$ ; an effect referred-to as noise-induced bistability (Horsthemke, 1984).

The effect of system size  $N$  in the mesoscopic description is captured in the stochastic term of (49), which is  $\mathcal{O}(1/\sqrt{N})$ . At small system sizes, the strength of stochasticity is relatively large and therefore, the order parameter is constantly pushed away from the stable equilibria  $m^* = \pm\sqrt{(h-4s)/h}$ . As a result, when  $N = 50$  we observe a relatively large spread around the two stable states in the distribution of  $m$  (see bottom row in Figure 4). On the other hand, for large system size the strength of stochasticity is less and thus system resides longer in the stable states. Consequently, the distribution shows two clear modes corresponding to deterministic stable equilibria in the system in low noise/large system size case.

We can explore the temporal evolution of the order parameter,  $m$ , by numerically integrating Eq (49) (— in Figure 4) or by Gillespie simulations (— in Figure 4). For small group sizes  $m$  does not reside evidently in the stable states, moving constantly across different states (top row of Figure 4). As the group size increases, the system resides longer in the two stable states ( $m^* = \pm\sqrt{\frac{h-4s}{h}}$ ), exhibiting occasional transitions between them. This effect was further quantified by Dyson et al. (2015) by calculating the mean residence time in the two stable states, which increases with group size. The results from all three approaches (the analytical approach, the SDE simulations and the Gillespie simulations) to solving the mesoscopic dynamics of the ternary interaction model qualitatively match with each other, with slight discrepancy for small groups sizes (Bottom row in Figure 4). This is not surprising since the Langevin and the Fokker-Planck equations approximates the dynamics for large but finite systems, but Gillespie simulations are exact representation of the underlying process.

## 5. Discussion

In this book chapter we presented two approaches from the literature, the system-size expansion method (Van Kampen, 1992) and the chemical Langevin equation method (Gillespie, 2000), to construct mesoscopic dynamical equations of collective behavior from microscopic rules. These methods allow us to capture how, for finite population sizes, stochasticity at the microscopic scale manifests at the mesoscopic scale. The resulting behaviour is captured by stochastic differential equations, sometimes referred to as Langevin equations. We demonstrated applications of these approaches to two simple models of collective decision-making involving individuals that must make a binary choice; in both cases, both methods yield identical Langevin equations. In the following Section 5.1 we therefore compare various technical aspects of the two complementary methods. In Section 5.2, we discuss how the aforementioned techniques reveal important differences regarding the two models we considered; one considers only pairwise interactions between individuals, whilst the other incorporates higher-order interactions. Finally, in Section 5.3, we discuss some extensions of the model.

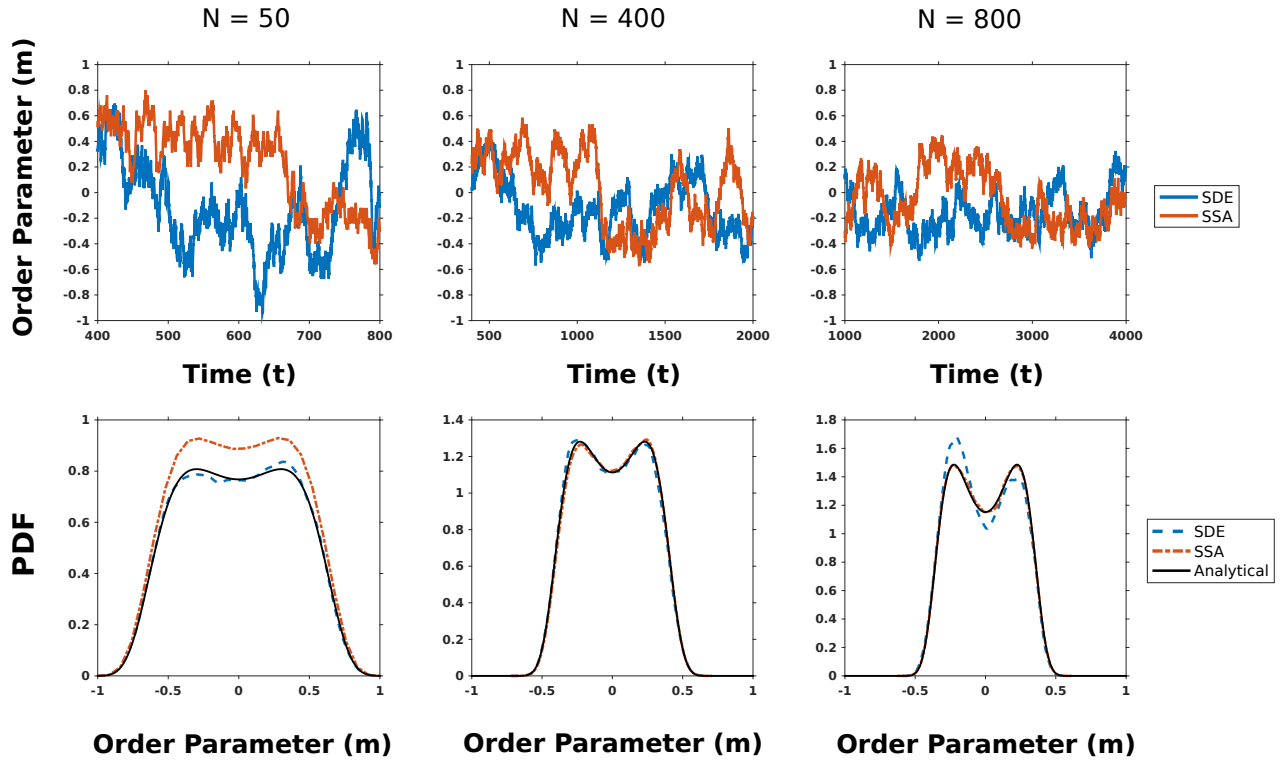


Figure 4: **Dynamics and steady state distributions of order parameter for the higher order interaction model** Top row: Time series of order parameter ( $m$ ) for three group size ( $N = 50, 400, 800$ ) from the numerical integration of the stochastic differential equation (sde) (49), shown in (—) and from the stochastic simulation algorithm (SSA) method (—). Bottom row: Corresponding steady state probability density functions of  $m$  obtained from numerical solutions of sde, SSA and the analytical solution of the Fokker-Planck equation (53), shown in (—). Parameter values:  $s = 0.05$ ,  $c = 0.005$ ,  $h = 0.21$

### 5.1. Comparison of system-size expansion with chemical Langevin approach

Both methods of constructing coarse-grained descriptions at mesoscopic scales are based on similar sets of assumptions. The system-size expansion method involves a formal procedure that begins with the master equation and then expands its terms in a small quantity: the inverse of the system size,  $1/N$ . By assuming  $N$  large and thereby keeping only two leading order terms, we obtain a Fokker-Planck equation, which describes the temporal evolution of the PDF of the order-parameter,  $m$ . This is equivalent to assuming that the rate-of-change in the probability distribution for  $m$  is fully determined by its first and second jump-moments, and hence that the noise is Gaussian in character. In contrast to this formal approach, the chemical Langevin method is based on heuristics that keep track of both the probability of each ‘chemical reaction’ (or interaction), and how each reaction changes the state of the system. To do this, the time-scale for reactions is so chosen that the changes in the number of individuals of each species can be approximated by a Gaussian/normal distribution. Thus, the two methods effectively make the same set of assumptions about the noise process that governs mesoscopic dynamics of the coarse-variable. [A more detailed discussion is provided in Gillespie (2002)]. Given this equivalence, it is not surprising that two methods do indeed yield identical Fokker-Planck equations and hence SDEs for the two univariate models under consideration.

More generally, the system-size expansion yields a Fokker-Planck equation, whilst the chemical Langevin approach results in one or more coupled SDEs. There is, of course, a formal equivalence between Fokker-Planck equations and SDEs. However, the decomposition of a Fokker-Planck equation into SDEs is not unique for multivariate systems. Specifically, this requires the decomposition of a known matrix—the matrix of second jump moments—into the product of an unknown matrix and its transpose. There exist many methods for such a decomposition, the Cholesky decomposition being a popular choice that ensures the unknown matrix is square but requires that the matrix of second jump moments is positive definite. In this case, the result is a set of coupled SDEs that involve the minimum number of possible noise sources (equal to the number of independent degrees-of-freedom required to fully describe the state of the system). By contrast, the chemical Langevin approach results in a system of coupled SDEs which involve as many noise sources as there are ‘chemical reactions’. Typically, the fewer noise terms of the Cholesky decomposition involve cumbersome and hard-to-simplify prefactors, whilst the many terms of the chemical Langevin equations have relatively straightforward prefactors. We demonstrate this point in Appendix B where we consider an extension of the binary-choice to four-choices, representing collective movement in two-dimensions rather than one. Using the system-size expansion to obtain a Fokker-Planck equation and then employing a Cholesky decomposition results in SDEs that are, for all intents and purposes, intractable, due to the complexity of the noise prefactors. However, by comparison, the chemical Langevin equations are significantly easier to construct and analyze.

We nevertheless stress that the two descriptions, as presented, *are* statistically the same, since they correspond to the same Fokker-Planck equation. The difference is purely aesthetic, and arises in multivariate systems due to the non-uniqueness of mapping a Fokker-Planck equation to a set of SDEs. However, one area, so far not discussed, where the two approaches do differ is the so-called Linear Noise Approximation (LNA) (Van Kampen, 1992). The LNA is attributed to van Kampen and typically used in conjunction with the expansion of transition rates in inverse system-size. It recognises that, formally, expansions of this type should be accompanied by an ansatz regarding the  $N$ -dependence of the underlying variables. If the variance of the underlying variables is expected to be proportional to  $\sqrt{N}$ , then this affects how the various terms of the expansion equate at lowest order, and results in mesoscopic descriptions that are *additive* in noise, rather than multiplicative. By contrast, if the variance is not expected to be Gaussian-like, then it does not affect the expansion at lowest order, and hence the LNA is not required.

### 5.2. Multiplicative noise at mesoscopic scales

To better understand the mesoscopic descriptions that result from the aforementioned approaches, we considered two simple models of collective behaviour from the literature, where individuals must make a binary choice between two alternatives. The models differ only in the way individuals interact. In the first case we assumed pairwise interactions (Kirman, 1993; Biancalani et al., 2014; Lux, 1995), whilst in the second case three individuals were permitted to interact at any given time (Dyson et al., 2015). In the literature, Biancalani et al. (2014) and Dyson et al. (2015) used the system-size expansion approach to derive mesoscopic equations for such models. Here, we recapitulate their results and, in addition, demonstrate the chemical Langevin equation approach; the latter having been used extensively for analyzing chemical reactions and biochemical networks, but much less in the ecology literature (Datta et al., 2010).

From this exercise, we may learn a number of interesting points about noise at mesoscopic scales. First and foremost, for the simple binary-choice models considered, the SDEs for the coarse-variable (consensus/order) contain multiplicative noise, *i.e.*, where the strength of stochasticity depends on the current state of the system. In other words, irrespective of the method of derivation, the resulting SDE is of the form  $dm/dt = f(m) + g(m)\eta(t)$ , with  $g(m) \neq \text{constant}$ . Secondly, studying these two models (both pairwise and ternary interactions) together provided an opportunity to highlight how the nature of interactions can subtly influence collective behaviour at mesoscopic scales. In both models, the noise term  $g(m)$  decreases with group size by  $\mathcal{O}(1/\sqrt{N})$ , however the effect of noise on collective behaviour contrasts sharply between the two. Perhaps counter-intuitively, increasing the strength of noise in the SDE of the pairwise interaction model, actually increases order, despite the ostensibly randomising effects of noise. This is exactly the opposite for the ternary interaction model, where increasing noise reduces the order, or level of consensus, among individuals.

To understand this quantitatively, consider the deterministic limit ( $N \rightarrow \infty$ ), in which  $dm/dt = f(m)$ . Here, we expect the system to asymptotically reach one of the deterministic stable states,  $m^*$ , given by  $f(m^*) = 0$  and  $f'(m^*) < 0$ . However, when the system is driven by multiplicative noise we have  $dm/dt = f(m) + g(m)\eta(t)$ , where the form of  $g(m)$  determines the most probable states of the system (Horsthemke, 1984). Crucially, these do *not* necessarily correspond to the deterministic stable states, as they would if the noise were simply additive [*i.e.*,  $g(m) = \text{constant}$ ]. This is precisely the case for the pairwise interaction model; the deterministic stable state corresponds to  $m^* = 0$ , but the most likely states (*i.e.*, the modes of the distribution) are close to  $m^* \pm 1$ . Thus, the multiplicative noise not only moves the system away from its deterministic stable state but also increases order. By contrast, in the higher-order (ternary) interaction model, the most likely states are indeed around or close to deterministic stable states.

### 5.3. Extensions and concluding remarks

In this chapter, we focussed only on two simple models of collective behaviour where interactions rules were either pairwise or at most ternary. Further, we focussed on non-spatial models and assumed that the system is fully-connected *i.e.* any individual can interact with any other individual. We deliberately chose these simple models because the main purpose of this chapter was to illustrate two complementary mathematical methods to deriving mesoscopic dynamics of the collective behaviour; elucidating how stochasticity arising from individual behaviours is amplified at mesoscopic scales by small group sizes.

An obvious extension of this work includes considering more complicated higher-order interactions; many empirical studies quantify nature of interactions suggest that interactions (Biro et al., 2006; Katz et al., 2011; Herbert-Read et al., 2011; Bialek et al., 2012; Gautrais et al., 2012; Mann et al.,

2013; Jiang et al., 2017) with some suggesting that interactions among flock-members can extend to several members, for example up to seven in starling flocks (Ballerini et al., 2008). For better representation of realistic flock dynamics, a continuous state/direction, which is in contrast to discrete states we have considered so far, could be incorporated (Othmer et al., 1988; Gavagnin and Yates, 2018). However, analysis of continuous state models may require more sophisticated analytical tools than presented in this chapter. Further, the emergence of collective behavior at mesoscopic scales, which is absent at macroscopic scales, is also of relevance to understand the evolution of collective behaviour. Much of the previous work concerning the evolution of social behaviour in animals has involved either deterministic game theory, which assumes infinite population sizes (Krause et al., 2002; Sumpter, 2010; Torney et al., 2010), or simulations of large numbers of particles (Reluga and Viscido, 2005; Spector et al., 2005; Wood and Ackland, 2007; Guttal and Couzin, 2010; Guttal et al., 2012). Recent studies have indeed begun to highlight the role of stochasticity arising from small group sizes and finite population sizes (Joshi et al., 2017; Joshi and Guttal, 2018) where mesoscopic descriptions are important.

Further, our assumption of fully-connected systems may be valid for small groups of animals, which is the focus of our paper, but for large groups, accounting for the local nature of interactions becomes important. Mesoscopic descriptions of such large but finite systems have been described for a small number of cases, and result in stochastic partial differential equations (Dean, 1996; Biancalani et al., 2010; McKane et al., 2014). On the other hand, the macroscopic or hydrodynamic descriptions of the collective motion models discussed in the first section have been well studied (Toner and Tu, 1995; Ramaswamy, 2010; Marchetti et al., 2013). It would therefore be interesting to understand how mesoscopic descriptions, which focus on capturing stochasticity arising from finite sized systems, dovetail with hydrodynamic descriptions at ostensibly larger length scales.

In summary, we presented two complementary approaches to derive mesoscopic descriptions of simple collective behaviour models. It is worth noting, however, that the methods we presented are applicable to any ecological model that are based on asynchronous stochastic update rules and where spatial structure is not important. For example, these methods can also be useful to deriving mesoscopic description of population and community dynamics which captures demographic stochasticity (Majumder, 2018). Whilst van Kampen’s system-size expansion has indeed been applied to study simple ecological and evolutionary scenarios (McKane and Newman, 2005; Traulsen et al., 2012; Black and McKane, 2012), we have highlighted the difficulty of employing this method for studying multi-species interactions. In such cases, we suggest that the method of chemical Langevin approach could be powerful. Therefore, we hope that our book chapter provides a pedagogical review of mathematical methods for describing mesoscopic dynamics that are useful not only for collective behaviour models but also for other biological dynamics where finite sizes of populations/groups is important.

## 6. Resources

The codes used for simulating the pairwise interaction and the ternary interaction models and the corresponding mesoscopic stochastic differential equations can be found at GitHub (<https://tinyurl.com/y8z>)

## 7. Acknowledgements

We thank Sabiha Majumder, Sumithra Sankaran, Jaideep Joshi, Jeffrey Phillipson, and Apilineni Kushal for various insightful discussions. We are thankful to Shubham Rana for useful comments on the manuscript. JJ acknowledges support by the Council for Scientific and Industrial



Research, India for research scholarship. RGM acknowledges support from Simons Foundation. VG acknowledges support from DBT-IISc partnership program, Science and Engineering Research Board (DST, Govt of India) and DST-FIST for infrastructure support.

## Appendix A. The Chemical Langevin equation

In this appendix, we briefly recapitulate the approach developed by Gillespie (2000). We consider  $n$  chemicals/species  $\{X_1, \dots, X_n\}$  whose interactions are represented via  $r$  chemical reactions  $\{R_1, \dots, R_r\}$ . We define the state of the system by  $\mathbf{N}(t) \equiv \{N_1(t), \dots, N_n(t)\}^\top$  where  $N_i(t)$  denotes the number of  $X_i$  molecules in the system at time  $t$ . Next, we define a propensity function  $a_j(\mathbf{N}(t))$ , which represents the probability that for a given state  $\mathbf{x}(t) = \mathbf{N}(t)/N$ , the reaction  $R_j$  will occur within the next infinitesimal time interval  $t + dt$ . Here,  $N = \sum_i N_i$  is the total number of individuals in the system. We also define the state change matrix  $\boldsymbol{\nu}_j$  whose  $i$ th component  $\nu_{ji}$  is defined by the change in the number of  $X_i$  molecules due to the occurrence of reaction  $R_j$ . For example, consider the reaction  $R_1 : X_1 + X_2 \rightarrow 2X_1$  and the reverse reaction  $R_2 : 2X_1 \rightarrow X_1 + X_2$ . The propensity function for the reaction  $R_1$  would be  $c_1 N_1 N_2 / N^2$ , and for the reaction  $R_2$  it would be  $c_2 N_1 (N_1 - 1) / 2N^2$ . The state change matrix would be  $\boldsymbol{\nu}_1 = (+1, -1, 0, \dots, 0)$ , such that  $\boldsymbol{\nu}_2 = -\boldsymbol{\nu}_1$ .

Gillespie (2000) points out that when two fairly generic dynamical conditions are satisfied, the propensity functions can be used to write down SDEs that describe the temporal evolution of the state variables  $\mathbf{x}$ , and hence a Fokker-Planck equation for  $P(\mathbf{x}, t)$ . Here, following Gillespie (2000), we present the most crucial steps and approximations for this derivation.

To write the time evolution of the PDF of  $\mathbf{N}$ —*i.e.*,  $P(\mathbf{N}, t | \mathbf{N}_0, t_0)$ —we consider a time scale sufficiently small that the probability of two or more reactions occurring is negligible compared to that of single reaction. We can then simply account for all the mutually exclusive ways of transitioning in-to or out-of state  $\mathbf{N}$  via zero or one reaction. The result is that the probability of the system being in state  $\mathbf{N}$  at time  $t + dt$  is given by:

$$P(\mathbf{N}, t+dt | \mathbf{N}_0, t_0) = P(\mathbf{N}, t | \mathbf{N}_0, t_0) \left[ 1 - \sum_{j=1}^r a_j(\mathbf{N}) dt \right] + \sum_{j=1}^r [P(\mathbf{N} - \boldsymbol{\nu}_j, t | \mathbf{N}_0, t_0) a_j(\mathbf{N} - \boldsymbol{\nu}_j) dt]. \quad (\text{A.1})$$

The first term in the above equation represents the probability that the system is already in state  $\mathbf{N}$  and no change occurs; this happens when none of the reactions,  $R_j$ , take place in the time interval  $[t, t + dt]$ , and corresponds to the probability  $1 - \sum_{j=1}^r a_j(\mathbf{N}) dt$ . The second term represents the probability that the system is in the state  $\mathbf{N}$  due to a jump from from one of the states  $\mathbf{N} - \boldsymbol{\nu}_j$  during the interval  $[t, t + dt]$ .

Rearranging the terms in Eq. (A.1) and taking the limit  $dt \rightarrow 0$  gives rise to the *chemical master equation*:

$$\frac{\partial}{\partial t} P(\mathbf{N}, t | \mathbf{N}_0, t_0) = \sum_{j=1}^r [P(\mathbf{N} - \boldsymbol{\nu}_j, t | \mathbf{N}_0, t_0) a_j(\mathbf{N} - \boldsymbol{\nu}_j) - P(\mathbf{N}, t | \mathbf{N}_0, t_0) a_j(\mathbf{N})]. \quad (\text{A.2})$$

In general, this integro-differential equation for the temporal evolution of  $P(\mathbf{N}, t | \mathbf{N}_0, t_0)$  is difficult to solve, which is why we seek a method to instead write down approximate (chemical) Langevin equations.

*Langevin Equations:* The state of the system after a time  $\tau$  has elapsed will depend on the number of reactions that have taken place during that time. Let  $K_j(\mathbf{N}, \tau)$  be the number of  $R_j$

reactions that occur in the time interval  $[t, t + \tau]$ . Since each  $R_j$  reaction contributes a change  $\nu_{ji}$  to the species  $X_i$ , the number of  $X_i$  molecules at time  $t + \tau$  will be

$$N_i(t + \tau) = N_i(t) + \sum_{j=1}^r K_j(\mathbf{N}, \tau) \nu_{ji}, \text{ for } i = 1, \dots, n. \quad (\text{A.3})$$

It is possible to approximate  $K_j(\mathbf{N}, \tau)$  for any  $\tau > 0$  when the following two conditions are satisfied: *Condition (i)*: The first condition requires  $\tau$  to be sufficiently small that none of the propensity functions change considerably, *i.e.*,

$$a_j(\mathbf{N}(t')) \cong a_j(\mathbf{N}(t)), \quad \forall t' \in [t, t + \tau], \quad \forall j \in [1, r]. \quad (\text{A.4})$$

This implies that we choose  $\tau$  such that none of the species concentrations change appreciably due to occurrence of any reaction, and that all the reaction events occur independently of each other in the time interval  $[t, t + \tau]$ . Moreover, the quantities  $K_j(\mathbf{N}, \tau)$ , the number of times each reaction occurs in this time interval, must be statistically independent Poisson random variables, denoted by  $\mathcal{P}_j(a_j(\mathbf{N}), \tau)$ . As a result, Eq. (A.3) can be approximated by

$$N_i(t + \tau) = N_i(t) + \sum_{j=1}^r \mathcal{P}_j(a_j(\mathbf{N}), \tau) \nu_{ji}, \text{ for } i = 1, \dots, n. \quad (\text{A.5})$$

*Condition (ii)*: In addition to the condition of  $\tau$  being sufficiently small, we require  $\tau$  to be large enough so that

$$\langle \mathcal{P}_j(a_j(\mathbf{N}), \tau) \rangle = a_j(\mathbf{N})\tau \gg 1. \quad (\text{A.6})$$

As a result, each Poisson random variable,  $\mathcal{P}_j(a_j(\mathbf{N}), \tau)$ , can be approximated by a *normal* random variable with a mean and a standard deviation both equal to  $a_j(\mathbf{N})\tau$ . We denote such a normal random variable by  $\mathcal{N}_j(a_j(\mathbf{N})\tau, a_j(\mathbf{N})\tau)$ , where the first argument indicates the mean and the second argument the variance. Therefore, Eq. (A.5) reduces to

$$N_i(t + \tau) = N_i(t) + \sum_{j=1}^r \mathcal{N}_j(a_j(\mathbf{N})\tau, a_j(\mathbf{N})\tau) \nu_{ji}, \text{ for } i = 1, \dots, n. \quad (\text{A.7})$$

Using the property that  $\mathcal{N}(m, \sigma^2) = m + \sigma\mathcal{N}(0, 1)$  and writing  $\mathcal{N}(0, 1) = \eta_j(t)$  for any  $t$ , we have

$$N_i(t + \tau) = N_i(t) + \sum_{j=1}^r \nu_{ji} a_j(\mathbf{N}) \tau + \sum_{j=1}^r \nu_{ji} [a_j(\mathbf{N}) \tau]^{1/2} \eta_j(t), \text{ for } i = 1, \dots, n. \quad (\text{A.8})$$

Let us denote  $\tau$  by  $dt$ , and formally consider the infinitesimal limit  $dt \rightarrow 0$ . We also note that  $\eta_j(t)$  and  $\eta_{j'}(t')$  are statistically uncorrelated for  $t \neq t'$  and  $j \neq j'$ , therefore,

$$\frac{dN_i(t)}{dt} = \sum_{j=1}^r \nu_{ji} a_j(\mathbf{N}) + \sum_{j=1}^r \nu_{ji} [a_j(\mathbf{N})]^{1/2} \eta_j(t), \text{ for } i = 1, \dots, n. \quad (\text{A.9})$$

Dividing the whole equation by  $N$  (total number of individuals in the system) and using the property that  $a_j(\mathbf{N}) = N a_j(\mathbf{x})$ , where  $\mathbf{x} = \mathbf{N}/N$  we finally arrive at the Langevin equations used in the main body of the Chapter:

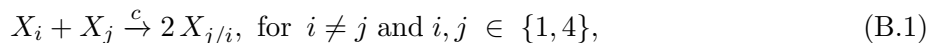
$$\frac{dx_i}{dt} = \sum_{j=1}^r \nu_{ji} a_j(\mathbf{x}) + \frac{1}{\sqrt{N}} \sum_{j=1}^r \nu_{ji} [a_j(\mathbf{x})]^{1/2} \eta_j(t), \text{ for } i = 1, \dots, n. \quad (\text{A.10})$$

## Appendix B. Pairwise interaction model in two spatial dimensions

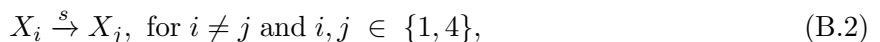
In this Appendix, we extend the pairwise interaction model to two spatial dimensions. As in the main body of the Chapter, we show how to construct coarse-grained equations for the dynamics of an order parameter from microscopic rules via two methods: (i) the system-size expansion method and (ii) the chemical Langevin equation approach. We show that, in contrast to the one-dimensional case, two spatial dimensions are enough to differentiate between the two approaches; the system-size expansion has significant limitations, whereas the CLE approach yields coarse-grained equations with relative ease.

Our starting point is to assume that individuals forage from four sources, located along the positive  $x$ , positive  $y$ , negative  $x$ , and negative  $y$  axes. We label these four perpendicular directions 1 to 4, respectively. We chose this discretization in lieu of a continuous two-dimensional space for reasons of analytical tractability; in a continuous two-dimensional system there are infinitely many directions along which individuals can move, and thus the number of states to consider are also infinite, prohibiting a straightforward extension of the methods we have discussed for the one-dimensional pairwise interaction model. [For examples of so-called ‘off-lattice’ techniques, see (Othmer et al., 1988; Dyson et al., 2012, 2015)].

As before, an ant moving in direction  $j$  is denoted by  $X_j$ . It changes its direction based on two types of reaction: a copying interaction



where  $c$  denotes the specific copying rate; and a spontaneous change in direction



where  $s$  denotes the specific spontaneous direction switching rate. The proportion of ants in each of the four directions, denoted by  $x_i$  for  $i \in \{1, 2, 3, 4\}$ , satisfy the constraint  $\sum_{i=1}^4 x_i = 1$ . We construct equations for the variable  $\mathbf{x} = \{x_1, x_2, x_3, x_4\}^T$ , representing the proportion of ants moving/foraging in the four different directions 1, ..., 4. We then calculate the group polarisation, or order parameter  $m = \sqrt{(x_1 - x_3)^2 + (x_2 - x_4)^2}$ . Each of the state variables  $x_i$  can take values in the range  $[0, 1]$ . The order parameter too, takes values from 0 to 1, with 0 representing disordered motion and 1 representing highly aligned motion, or consensus among ants for the foraging source.

### Appendix B.1. van-Kampen’s system-size expansion of transition rates

*Transition rates:* Using the shorthand notation  $x_i^+ = x_i + 1/N$  and  $x_j^- = x_j - 1/N$ , the transition rates are the same as for the one dimensional case

$$T_{ij}(\mathbf{x}) = T(x_i^+, x_j^- | x_i, x_j) = cx_i x_j + sx_j, \quad (\text{B.3})$$

except the indices can now take the values 1, 2, 3, 4.

*Master Equation:* The corresponding master equation is then just

$$\frac{\partial P(\mathbf{x}, t)}{\partial t} = \sum_i \sum_{j \neq i} \left[ P(x_i^+, x_j^-) T(x_i, x_j | x_i^+, x_j^-) - P(x_i, x_j) T(x_i^+, x_j^- | x_i, x_j) \right]. \quad (\text{B.4})$$

As before, this can be simplified by using the step operators  $\mathcal{E}_i^+$  and  $\mathcal{E}_i^-$ , such that

$$\mathcal{E}_i^\pm(x_i) = f(x_i \pm 1/N) = f(x_i^\pm), \quad (\text{B.5})$$

whereby the master equation may be re-written to give

$$\frac{\partial P(\mathbf{x}, t)}{\partial t} = \sum_i \sum_{j \neq i} (\mathcal{E}_i^- \mathcal{E}_j^+ - 1) P(\mathbf{x}, t) T_{ij}. \quad (\text{B.6})$$

*Fokker-Planck Equation:* Assuming a large-but-finite  $N$ , we approximate the action of the step-operators via Taylor expansion. Ignoring terms at  $O(1/N^3)$ , we have

$$\mathcal{E}_i^+ f(x_i) = f\left(x_i + \frac{1}{N}\right) = \left(1 + \frac{1}{N} \frac{\partial}{\partial x_i} + \frac{1}{2N^2} \frac{\partial^2}{\partial x_i^2}\right) f(x_i), \quad (\text{B.7a})$$

$$\mathcal{E}_i^- f(x_i) = f\left(x_i - \frac{1}{N}\right) = \left(1 - \frac{1}{N} \frac{\partial}{\partial x_i} + \frac{1}{2N^2} \frac{\partial^2}{\partial x_i^2}\right) f(x_i), \quad (\text{B.7b})$$

and therefore

$$\mathcal{E}_i^- \mathcal{E}_j^+ = 1 + \frac{1}{N} \left( \frac{\partial}{\partial x_j} - \frac{\partial}{\partial x_i} \right) + \frac{1}{2N^2} \left( \frac{\partial}{\partial x_j} - \frac{\partial}{\partial x_i} \right)^2. \quad (\text{B.8})$$

Substituting into (B.6), rearranging and making the substitution  $t = N\tau$ , we get the generic Fokker-Planck equation

$$\frac{\partial P(\mathbf{x})}{\partial \tau} = - \sum_{i=1}^{n-1} \frac{\partial}{\partial x_i} P(\mathbf{x}) A_i(\mathbf{x}) + \frac{1}{2} \sum_{i,j=1}^{n-1} \frac{\partial^2}{\partial x_i \partial x_j} P(\mathbf{x}) B_{ij}(\mathbf{x}), \quad (\text{B.9})$$

where  $n = 4$  is the total number of states/directions/food sources. Due to the constraint  $\sum_{i=1}^4 x_i = 1$ , we require only three variables to determine the state of the system, and the deterministic vector  $\mathcal{A}(\mathbf{x})$  therefore has three elements

$$\mathcal{A}_i(\mathbf{x}) = \sum_{j \neq i}^3 [T_{ij}(\mathbf{x}) - T_{ji}(\mathbf{x})], \text{ for } i = 1, \dots, 3. \quad (\text{B.10})$$

Similarly, the matrix  $\mathcal{B}(\mathbf{x})$  is a  $3 \times 3$ , whose off-diagonal and diagonal elements, respectively, are given by

$$\mathcal{B}_{ij}(\mathbf{x}) = -\frac{1}{N} [T_{ij}(\mathbf{x}) + T_{ji}(\mathbf{x})], \text{ for } i \neq j, \quad (\text{B.11})$$

$$\mathcal{B}_{ii}(\mathbf{x}) = \frac{1}{N} \sum_{j \neq i} [T_{ij}(\mathbf{x}) + T_{ji}(\mathbf{x})]. \quad (\text{B.12})$$

For the pairwise interaction model in two dimensions represented by (B.1) and (B.2),  $\mathcal{A}$  and  $\mathcal{B}$  are given by

$$\mathcal{A}_i(\mathbf{x}) = s(1 - 4x_i),$$

$$\mathcal{B}_{ij}(\mathbf{x}) = -\frac{1}{N} [s(x_i + x_j) + 2cx_i x_j],$$

and

$$\mathcal{B}_{ii}(\mathbf{x}) = \frac{1}{N} [s(1 + 2x_i) + 2c \sum_{j \neq i} x_i x_j].$$

*Mesoscopic SDEs:* Given a multivariate Fokker-Planck equation of the form B.9, we can write the corresponding SDEs as follows (Gardiner, 2009)

$$\frac{dx_i}{dt} = \mathcal{A}_i(\mathbf{x}) + \sum_{j=1}^{n-1} \mathcal{G}_{ij}(\mathbf{x})\eta_j(\tau), \quad (\text{B.13})$$

where the  $\eta_j$  ( $j = 1, 2, 3$ ) represent uncorrelated Gaussian white noise sources, and the matrix  $\mathcal{G}$  is defined by the relation  $\mathcal{G}\mathcal{G}^T = \mathcal{B}$ . Since all  $x_i$  are real, the matrix  $\mathcal{G}$  must necessarily be real; the condition for which is that  $\mathcal{B}$  is positive definite—*i.e.*, all the eigenvalues of  $\mathcal{B}$  are real and positive. For the pairwise interaction model in two dimensions, we find that this condition does not hold. Numerically, we find that one of the eigenvalues of  $\mathcal{B}$  is always zero, suggesting that  $\mathcal{B}$  is positive *semi*-definite, and therefore  $\mathcal{G}$  is not unique. We conclude, therefore, that deriving analytically tractable mesoscopic equations is not feasible for the two dimensional pairwise interaction model using the van Kampen’s method of system-size expansion. In the next subsection we describe the chemical Langevin equation method, which allows us to write-down a coupled set of SDEs directly from the microscopic reactions.

### Appendix B.2. Chemical Langevin approach

Based on the scheme of reactions in Eqs. (B.1) and (B.2), we have 12 copying reactions and 12 spontaneous switching reactions. Each of these reactions result in a change in state, such as  $x_i \rightarrow x_i + 1/N$  and  $x_j \rightarrow x_j - 1/N$ , for various combinations of  $i \neq j$ . For these 24 different reactions, we can write both propensity functions for the probability of each reaction and a state change vector  $\nu_{ji}$ , to capture the ‘stoichiometry’ of the reactions. We show all the reactions with their propensity functions and corresponding state change vector entries in Table B.2. Using these details, we show how to write the CLE for the state  $x_1$ , such that the method can easily be applied to the remaining states. We recall that the generic form of a CLE is given by

$$\frac{dx_i}{dt} = \sum_{j=1}^r \nu_{ji} a_j(\mathbf{x}) + \frac{1}{\sqrt{N}} \sum_{j=1}^r \nu_{ji} a_j(\mathbf{x})^{1/2} \eta_j(t), \quad (\text{B.14})$$

Substituting the values of  $\nu_{ji}$  and  $a_j(\mathbf{x})$  for  $i = 1$  from Table B.2 into the above equation we see that

$$\begin{aligned} \sum_{j=1}^r \nu_{j1} a_j(\mathbf{x}(t)) &= cx_1x_2 - cx_1x_2 + cx_1x_3 - cx_1x_3 + cx_1x_4 - cx_1x_4 - sx_1 + sx_2 - sx_1 + sx_3 - sx_1 + sx_4, \\ &= s(x_2 - x_1) + s(x_3 - x_1) + s(x_4 - x_1), \\ &= s(1 - 4x_1). \end{aligned}$$

And similarly,

$$\begin{aligned} \sum_{j=1}^r \nu_{j1} [a_j(\mathbf{x}(t))]^{1/2} &= \sqrt{cx_1x_2}\eta_1 - \sqrt{cx_1x_2}\eta_2 + \sqrt{cx_1x_3}\eta_3 - \sqrt{cx_1x_3}\eta_4 + \sqrt{cx_1x_4}\eta_5 - \sqrt{cx_1x_4}\eta_6 \\ &\quad - \sqrt{sx_1}\eta_{13} + \sqrt{sx_2}\eta_{14} - \sqrt{sx_1}\eta_{15} + \sqrt{sx_3}\eta_{16} - \sqrt{sx_1}\eta_{17} + \sqrt{sx_4}\eta_{18}, \end{aligned}$$

which results in the following SDE for the variable  $x_1$ :

$$\begin{aligned} \frac{dx_1}{dt} &= s(1 - 4x_1) + \frac{1}{\sqrt{N}} (\sqrt{cx_1x_2}\eta_1 - \sqrt{cx_1x_2}\eta_2 + \sqrt{cx_1x_3}\eta_3 - \sqrt{cx_1x_3}\eta_4 + \sqrt{cx_1x_4}\eta_5 - \sqrt{cx_1x_4}\eta_6 \\ &\quad - \sqrt{sx_1}\eta_{13} + \sqrt{sx_2}\eta_{14} - \sqrt{sx_1}\eta_{15} + \sqrt{sx_3}\eta_{16} - \sqrt{sx_1}\eta_{17} + \sqrt{sx_4}\eta_{18}), \end{aligned} \quad (\text{B.15})$$

S. No. (j)	Reaction	Propensity	$\nu_{j1}$	$\nu_{j2}$	$\nu_{j3}$	$\nu_{j4}$
1	$X_1 + X_2 \xrightarrow{c} 2X_1$	$cx_1x_2$	1	-1	0	0
2	$X_2 + X_1 \xrightarrow{c} 2X_2$	$cx_1x_2$	-1	1	0	0
3	$X_1 + X_3 \xrightarrow{c} 2X_1$	$cx_1x_3$	1	0	-1	0
4	$X_3 + X_1 \xrightarrow{c} 2X_3$	$cx_1x_3$	-1	0	1	0
5	$X_1 + X_4 \xrightarrow{c} 2X_1$	$cx_1x_4$	1	0	0	-1
6	$X_4 + X_1 \xrightarrow{c} 2X_4$	$cx_1x_4$	-1	0	0	1
7	$X_2 + X_3 \xrightarrow{c} 2X_2$	$cx_2x_3$	0	1	-1	0
8	$X_3 + X_2 \xrightarrow{c} 2X_3$	$cx_2x_3$	0	-1	1	0
9	$X_2 + X_4 \xrightarrow{c} 2X_2$	$cx_2x_4$	0	1	0	-1
10	$X_4 + X_2 \xrightarrow{c} 2X_4$	$cx_2x_4$	0	-1	0	1
11	$X_3 + X_4 \xrightarrow{c} 2X_3$	$cx_3x_4$	0	0	1	-1
12	$X_4 + X_3 \xrightarrow{c} 2X_4$	$cx_3x_4$	0	0	-1	1
13	$X_1 \xrightarrow{s} X_2$	$sx_1$	-1	1	0	0
14	$X_2 \xrightarrow{s} X_1$	$sx_2$	1	-1	0	0
15	$X_1 \xrightarrow{s} X_3$	$sx_1$	-1	0	1	0
16	$X_3 \xrightarrow{s} X_1$	$sx_3$	1	0	-1	0
17	$X_1 \xrightarrow{s} X_4$	$sx_1$	-1	0	0	1
18	$X_4 \xrightarrow{s} X_1$	$sx_4$	1	0	0	-1
19	$X_2 \xrightarrow{s} X_3$	$sx_2$	0	-1	1	0
20	$X_3 \xrightarrow{s} X_2$	$sx_3$	0	1	-1	0
21	$X_2 \xrightarrow{s} X_4$	$sx_2$	0	-1	0	1
22	$X_4 \xrightarrow{s} X_2$	$sx_4$	0	1	0	-1
23	$X_3 \xrightarrow{s} X_4$	$sx_3$	0	0	-1	1
24	$X_4 \xrightarrow{s} X_3$	$sx_4$	0	0	1	-1

Table B.2: Reactions in the pairwise interaction model in two dimensions and their propensities and state change vector

Performing the similar substitutions for the remaining variables results in

$$\begin{aligned} \frac{dx_2}{dt} = s(1 - 4x_2) + \frac{1}{\sqrt{N}} & (\sqrt{cx_1x_2}\eta_2 - \sqrt{cx_1x_2}\eta_1 + \sqrt{cx_2x_3}\eta_7 - \sqrt{cx_2x_3}\eta_8 + \sqrt{cx_2x_4}\eta_9 - \sqrt{cx_2x_4}\eta_{10} \\ & + \sqrt{sx_1}\eta_{13} - \sqrt{sx_2}\eta_{14} - \sqrt{sx_2}\eta_{19} + \sqrt{sx_3}\eta_{20} - \sqrt{sx_2}\eta_{21} + \sqrt{sx_4}\eta_{22}), \end{aligned} \quad (\text{B.16a})$$

$$\begin{aligned} \frac{dx_3}{dt} = s(1 - 4x_3) + \frac{1}{\sqrt{N}} & (\sqrt{cx_1x_3}\eta_4 - \sqrt{cx_1x_3}\eta_3 + \sqrt{cx_2x_3}\eta_8 - \sqrt{cx_2x_3}\eta_7 + \sqrt{cx_3x_4}\eta_{11} - \sqrt{cx_3x_4}\eta_{12} \\ & + \sqrt{sx_1}\eta_{15} - \sqrt{sx_3}\eta_{16} + \sqrt{sx_2}\eta_{19} - \sqrt{sx_3}\eta_{20} - \sqrt{sx_3}\eta_{23} + \sqrt{sx_4}\eta_{24}), \end{aligned} \quad (\text{B.16b})$$

$$\begin{aligned} \frac{dx_4}{dt} = s(1 - 4x_4) + \frac{1}{\sqrt{N}} & (\sqrt{cx_1x_4}\eta_6 - \sqrt{cx_1x_4}\eta_5 + \sqrt{cx_2x_4}\eta_{10} - \sqrt{cx_2x_4}\eta_9 + \sqrt{cx_3x_4}\eta_{12} - \sqrt{cx_3x_4}\eta_{11} \\ & + \sqrt{sx_1}\eta_{17} - \sqrt{sx_4}\eta_{18} + \sqrt{sx_2}\eta_{21} - \sqrt{sx_4}\eta_{22} + \sqrt{sx_3}\eta_{23} - \sqrt{sx_4}\eta_{24}), \end{aligned} \quad (\text{B.16c})$$

where,  $\eta_1, \eta_2, \dots, \eta_{24}$  are delta-correlated Gaussian white noise sources. Unfortunately, further simplification of the stochastic terms is not possible in this case because the coupled nature of the equations. Nevertheless, the corresponding multivariate Fokker-Planck equation can be derived by following Gillespie (2002).

$$\begin{aligned} \frac{\partial P(\mathbf{x}, t | \mathbf{x}_0, t_0)}{\partial t} = & - \sum_{i=1}^n \frac{\partial}{\partial x_i} \left[ \left( \sum_{j=1}^r \nu_{ji} a_j(\mathbf{x}) \right) P(\mathbf{x}, t | \mathbf{x}_0, t_0) \right] \\ & + \frac{1}{2N} \sum_{i=1}^n \frac{\partial^2}{\partial x_i^2} \left[ \left( \sum_{j=1}^r \nu_{ji}^2 a_j(\mathbf{x}) \right) P(\mathbf{x}, t | \mathbf{x}_0, t_0) \right] \\ & + \frac{1}{N} \sum_{i'=1}^n \sum_{i < i'} \frac{\partial^2}{\partial x_i \partial x_{i'}} \left[ \left( \sum_{j=1}^r \nu_{ji} \nu_{ji'} a_j(\mathbf{x}) \right) P(\mathbf{x}, t | \mathbf{x}_0, t_0) \right]. \end{aligned} \quad (\text{B.17})$$

Substituting the values of  $\nu_{ji}$  and  $a_j(\mathbf{x})$  from Table B.2 recovers a Fokker-Planck equation, of the form

$$\frac{\partial P(\mathbf{x})}{\partial \tau} = - \sum_{i=1}^n \frac{\partial}{\partial x_i} [P(\mathbf{x}) \mathcal{A}_i(\mathbf{x})] + \frac{1}{2} \sum_{i,j=1}^n \frac{\partial^2}{\partial x_i \partial x_j} [P(\mathbf{x}) \mathcal{B}_{ij}(\mathbf{x})], \quad (\text{B.18})$$

where  $\mathcal{A}(\mathbf{x})$  is given by

$$\mathcal{A}_i(\mathbf{x}) = s(1 - 4x_i),$$

whilst the diagonal and off-diagonal elements of  $\mathcal{B}(\mathbf{x})$  are given by

$$\mathcal{B}_{ii}(\mathbf{x}) = \frac{1}{N} [s(1 + 2x_i) + 2c \sum_{j \neq i} x_i x_j],$$

and

$$\mathcal{B}_{ij}(\mathbf{x}) = -\frac{1}{N} [s(x_i + x_j) + 2cx_i x_j],$$

respectively. This is the same Fokker-Planck equation as derived using system-size expansion.

## References

## References

- Aldana, M., Dossetti, V., Huepe, C., Kenkre, V., Larralde, H., 2007. Phase transitions in systems of self-propelled agents and related network models. *Physical review letters* 98 (9), 095702.
- Alfarano, S., Lux, T., Wagner, F., 2008. Time variation of higher moments in a financial market with heterogeneous agents: An analytical approach. *Journal of Economic Dynamics and Control* 32 (1), 101–136.
- Altschuler, S. J., Angenent, S. B., Wang, Y., Wu, L. F., 2008. On the spontaneous emergence of cell polarity. *Nature* 454 (7206), 886.
- Attanasi, A., Cavagna, A., Del Castello, L., Giardina, I., Grigera, T. S., Jelić, A., Melillo, S., Parisi, L., Pohl, O., Shen, E., et al., 2014. Information transfer and behavioural inertia in starling flocks. *Nature physics* 10 (9), 691.
- Baglietto, G., Albano, E. V., 2009. Nature of the order-disorder transition in the vicsek model for the collective motion of self-propelled particles. *Physical Review E* 80 (5), 050103.
- Ballerini, M., Cabibbo, N., Candelier, R., Cavagna, A., Cisbani, E., Giardina, I., Lecomte, V., Orlandi, A., Parisi, G., Procaccini, A., et al., 2008. Interaction ruling animal collective behavior depends on topological rather than metric distance: Evidence from a field study. *Proceedings of the national academy of sciences* 105 (4), 1232–1237.
- Beckers, R., Deneubourg, J.-L., Goss, S., Pasteels, J. M., 1990. Collective decision making through food recruitment. *Insectes sociaux* 37 (3), 258–267.
- Berdahl, A., Torney, C. J., Ioannou, C. C., Faria, J. J., Couzin, I. D., 2013. Emergent sensing of complex environments by mobile animal groups. *Science* 339 (6119), 574–576.
- Bialek, W., Cavagna, A., Giardina, I., Mora, T., Silvestri, E., Viale, M., Walczak, A. M., 2012. Statistical mechanics for natural flocks of birds. *Proceedings of the National Academy of Sciences*.
- Biancalani, T., Dyson, L., McKane, A. J., 2014. Noise-induced bistable states and their mean switching time in foraging colonies. *Physical review letters* 112 (3), 038101.
- Biancalani, T., Fanelli, D., Di Patti, F., 2010. Stochastic turing patterns in the brusselator model. *Physical Review E* 81 (4), 046215.
- Biro, D., Sumpter, D. J., Meade, J., Guilford, T., 2006. From compromise to leadership in pigeon homing. *Current Biology* 16 (21), 2123–2128.
- Black, A. J., McKane, A. J., 2012. Stochastic formulation of ecological models and their applications. *Trends in ecology & evolution* 27 (6), 337–345.
- Boettiger, C., 2018. From noise to knowledge: how randomness generates novel phenomena and reveals information. *Ecology letters* 21 (8), 1255–1267.
- Bonabeau, E., Theraulaz, G., Deneubourg, J.-L., Aron, S., Camazine, S., 1997. Self-organization in social insects. *Trends in Ecology & Evolution* 12 (5), 188–193.



- Buhl, J., Sumpter, D. J., Couzin, I. D., Hale, J. J., Despland, E., Miller, E. R., Simpson, S. J., 2006. From disorder to order in marching locusts. *Science* 312 (5778), 1402–1406.
- Camazine, S., Deneubourg, J.-L., Franks, N. R., Sneyd, J., Bonabeau, E., Theraula, G., 2003. *Self-organization in biological systems*. Vol. 7. Princeton University Press.
- Cavagna, A., Cimarelli, A., Giardina, I., Parisi, G., Santagati, R., Stefanini, F., Viale, M., 2010. Scale-free correlations in starling flocks. *Proceedings of the National Academy of Sciences* 107 (26), 11865–11870.
- Chaté, H., Ginelli, F., Grégoire, G., Raynaud, F., 2008. Collective motion of self-propelled particles interacting without cohesion. *Physical Review E* 77 (4), 046113.
- Chowdhury, D., Guttal, V., Nishinari, K., Schadschneider, A., 2002. A cellular-automata model of flow in ant trails: non-monotonic variation of speed with density. *Journal of Physics A: Mathematical and General* 35 (41), L573.
- Colizza, V., Barrat, A., Barthelemy, M., Valleron, A.-J., Vespignani, A., 2007. Modeling the worldwide spread of pandemic influenza: baseline case and containment interventions. *PLoS medicine* 4 (1), e13.
- Couzin, I. D., Krause, J., Franks, N. R., Levin, S. A., 2005. Effective leadership and decision-making in animal groups on the move. *Nature* 433 (7025), 513.
- Couzin, I. D., Krause, J., James, R., Ruxton, G. D., Franks, N. R., 2002. Collective memory and spatial sorting in animal groups. *Journal of theoretical biology* 218 (1), 1–11.
- Cox, J. T., Griffeath, D., 1986. Diffusive clustering in the two dimensional voter model. *The Annals of Probability* 14 (2), 347–370.
- Czirók, A., Barabási, A.-L., Vicsek, T., 1999a. Collective motion of self-propelled particles: Kinetic phase transition in one dimension. *Physical Review Letters* 82 (1), 209.
- Czirók, A., Vicsek, M., Vicsek, T., 1999b. Collective motion of organisms in three dimensions. *Physica A: Statistical Mechanics and its Applications* 264 (1-2), 299–304.
- Datta, S., Delius, G. W., Law, R., 2010. A jump-growth model for predator–prey dynamics: derivation and application to marine ecosystems. *Bulletin of mathematical biology* 72 (6), 1361–1382.
- Dean, D. S., 1996. Langevin equation for the density of a system of interacting langevin processes. *Journal of Physics A: Mathematical and General* 29 (24), L613.
- Deneubourg, J.-L., Goss, S., 1989. Collective patterns and decision-making. *Ethology Ecology & Evolution* 1 (4), 295–311.
- Dussutour, A., Nicolis, S. C., Deneubourg, J.-L., Fourcassié, V., 2006. Collective decisions in ants when foraging under crowded conditions. *Behavioral Ecology and Sociobiology* 61 (1), 17–30.
- Dyson, L., Maini, P. K., Baker, R. E., 2012. Macroscopic limits of individual-based models for motile cell populations with volume exclusion. *Physical Review E* 86 (3), 031903.
- Dyson, L., Yates, C. A., Buhl, J., McKane, A. J., 2015. Onset of collective motion in locusts is captured by a minimal model. *Physical Review E* 92 (5), 052708.

- El-Samad, H., Prajna, S., Papachristodoulou, A., Doyle, J., Khammash, M., 2006. Advanced methods and algorithms for biological networks analysis. *Proceedings of the IEEE* 94 (4), 832–853.
- Erban, R., Chapman, S. J., 2009. Stochastic modelling of reaction–diffusion processes: algorithms for bimolecular reactions. *Physical biology* 6 (4), 046001.
- Flierl, G., Grünbaum, D., Levins, S., Olson, D., 1999. From individuals to aggregations: the interplay between behavior and physics. *Journal of Theoretical biology* 196 (4), 397–454.
- Franks, N. R., Wilby, A., Silverman, B. W., Tofts, C., 1992. Self-organizing nest construction in ants: sophisticated building by blind bulldozing. *Animal behaviour* 44, 357–375.
- Gardiner, C., 2009. *Stochastic methods*. Vol. 4. Springer Berlin.
- Gautrais, J., Ginelli, F., Fournier, R., Blanco, S., Soria, M., Chaté, H., Theraulaz, G., 2012. Deciphering interactions in moving animal groups. *Plos computational biology* 8 (9), e1002678.
- Gavagnin, E., Yates, C. A., 2018. Stochastic and deterministic modelling of cell migration. arXiv preprint arXiv:1806.06724.
- Gillespie, D. T., 1976. A general method for numerically simulating the stochastic time evolution of coupled chemical reactions. *Journal of computational physics* 22 (4), 403–434.
- Gillespie, D. T., 1977. Exact stochastic simulation of coupled chemical reactions. *The journal of physical chemistry* 81 (25), 2340–2361.
- Gillespie, D. T., 2000. The chemical langevin equation. *The Journal of Chemical Physics* 113 (1), 297–306.
- Gillespie, D. T., 2001. Approximate accelerated stochastic simulation of chemically reacting systems. *The Journal of Chemical Physics* 115 (4), 1716–1733.
- Gillespie, D. T., 2002. The chemical langevin and fokker- planck equations for the reversible isomerization reaction. *The Journal of Physical Chemistry A* 106 (20), 5063–5071.
- Ginelli, F., 2016. The physics of the vicsek model. *The European Physical Journal Special Topics* 225 (11-12), 2099–2117.
- Gordon, D. M., 1996. The organization of work in social insect colonies. *Nature* 380 (6570), 121.
- Grégoire, G., Chaté, H., 2004. Onset of collective and cohesive motion. *Physical review letters* 92 (2), 025702.
- Grünbaum, D., 1998. Schooling as a strategy for taxis in a noisy environment. *Evolutionary Ecology* 12 (5), 503–522.
- Guttal, V., 2014. Ecology: From individuals to collectives. *Resonance* 19 (4), 368–375.
- Guttal, V., Couzin, I. D., 2010. Social interactions, information use, and the evolution of collective migration. *Proceedings of the national academy of sciences* 107 (37), 16172–16177.
- Guttal, V., Romanczuk, P., Simpson, S. J., Sword, G. A., Couzin, I. D., 2012. Cannibalism can drive the evolution of behavioural phase polyphenism in locusts. *Ecology letters* 15 (10), 1158–1166.

- Herbert-Read, J. E., Perna, A., Mann, R. P., Schaerf, T. M., Sumpter, D. J., Ward, A. J., 2011. Inferring the rules of interaction of shoaling fish. *Proceedings of the National Academy of Sciences* 108 (46), 18726–18731.
- Horsthemke, W., 1984. Noise induced transitions. In: *Non-Equilibrium Dynamics in Chemical Systems*. Springer, pp. 150–160.
- Inada, Y., Kawachi, K., 2002. Order and flexibility in the motion of fish schools. *Journal of theoretical Biology* 214 (3), 371–387.
- Jadbabaie, A., Lin, J., Morse, A. S., 2003. Coordination of groups of mobile autonomous agents using nearest neighbor rules. *IEEE Transactions on automatic control* 48 (6), 988–1001.
- Jiang, L., Giuggioli, L., Perna, A., Escobedo, R., Lecheval, V., Sire, C., Han, Z., Theraulaz, G., 2017. Identifying influential neighbors in animal flocking. *PLoS Computational Biology* 13 (11), 1 – 32.
- Joshi, J., Couzin, I. D., Levin, S. A., Guttal, V., 2017. Mobility can promote the evolution of cooperation via emergent self-assortment dynamics. *PLoS computational biology* 13 (9), e1005732.
- Joshi, J., Guttal, V., 2018. Demographic noise and cost of greenbeard can facilitate greenbeard cooperation. *Evolution* 72 (12), 2595–2607.
- Katz, Y., Tunstrøm, K., Ioannou, C. C., Huepe, C., Couzin, I. D., 2011. Inferring the structure and dynamics of interactions in schooling fish. *Proceedings of the National Academy of Sciences* 108 (46), 18720–18725.
- Kimura, M., Weiss, G. H., 1964. The stepping stone model of population structure and the decrease of genetic correlation with distance. *Genetics* 49 (4), 561–576.
- Kirman, A., 1993. Ants, rationality, and recruitment. *The Quarterly Journal of Economics* 108 (1), 137–156.
- Kolpas, A., 2008. Coarse-grained analysis of collective motion in animal groups [dissertation]. University of California, Santa Barbara.
- Kolpas, A., Moehlis, J., Kevrekidis, I. G., 2007. Coarse-grained analysis of stochasticity-induced switching between collective motion states. *Proceedings of the National Academy of Sciences* 104 (14), 5931–5935.
- Krause, J., Ruxton, G. D., Ruxton, G. D., 2002. *Living in groups*. Oxford University Press.
- Kunwar, A., John, A., Nishinari, K., Schadschneider, A., Chowdhury, D., 2004. Collective traffic-like movement of ants on a trail: dynamical phases and phase transitions. *Journal of the Physical Society of Japan* 73 (11), 2979–2985.
- Lawson, M. J., Drawert, B., Khammash, M., Petzold, L., Yi, T.-M., 2013. Spatial stochastic dynamics enable robust cell polarization. *PLoS computational biology* 9 (7), e1003139.
- Lux, T., 1995. Herd behaviour, bubbles and crashes. *The economic journal* 105 (431), 881–896.
- Majumder, S., 2018. Multiple stable states and abrupt transitions in spatial ecosystems [dissertation]. Indian Institute of Science, Bangalore.

- Mann, R. P., Perna, A., Strömbom, D., Garnett, R., Herbert-Read, J. E., Sumpter, D. J., Ward, A. J., 2013. Multi-scale inference of interaction rules in animal groups using bayesian model selection. *PLoS computational biology* 9 (3), e1002961.
- Marchetti, M. C., Joanny, J.-F., Ramaswamy, S., Liverpool, T. B., Prost, J., Rao, M., Simha, R. A., 2013. Hydrodynamics of soft active matter. *Reviews of Modern Physics* 85 (3), 1143.
- McKane, A. J., Biancalani, T., Rogers, T., 2014. Stochastic pattern formation and spontaneous polarisation: the linear noise approximation and beyond. *Bulletin of mathematical biology* 76 (4), 895–921.
- McKane, A. J., Newman, T. J., 2004. Stochastic models in population biology and their deterministic analogs. *Physical Review E* 70 (4), 041902.
- McKane, A. J., Newman, T. J., 2005. Predator-prey cycles from resonant amplification of demographic stochasticity. *Physical review letters* 94 (21), 218102.
- Mogilner, A., Edelstein-Keshet, L., 1999. A non-local model for a swarm. *Journal of Mathematical Biology* 38 (6), 534–570.
- Nishinari, K., Sugawara, K., Kazama, T., Schadschneider, A., Chowdhury, D., 2006. Modelling of self-driven particles: Foraging ants and pedestrians. *Physica A: Statistical Mechanics and its Applications* 372 (1), 132–141.
- Othmer, H. G., Dunbar, S. R., Alt, W., 1988. Models of dispersal in biological systems. *Journal of mathematical biology* 26 (3), 263–298.
- Parrish, J. K., Viscido, S. V., Grunbaum, D., 2002. Self-organized fish schools: an examination of emergent properties. *The biological bulletin* 202 (3), 296–305.
- Petit, O., Bon, R., 2010. Decision-making processes: the case of collective movements. *Behavioural Processes* 84 (3), 635–647.
- Pratt, S. C., Mallon, E. B., Sumpter, D. J., Franks, N. R., 2002. Quorum sensing, recruitment, and collective decision-making during colony emigration by the ant *leptothorax albipennis*. *Behavioral Ecology and Sociobiology* 52 (2), 117–127.
- Press, W. H., Teukolsky, S. A., Vetterling, W. T., Flannery, B. P., 1996. *Numerical recipes in C. Vol. 2.* Cambridge university press Cambridge.
- Ramaswamy, S., 2010. The mechanics and statistics of active matter. *The Annual Review of Condensed Matter Physics* 1, 323–45.
- Reluga, T. C., Viscido, S., 2005. Simulated evolution of selfish herd behavior. *Journal of Theoretical Biology* 234 (2), 213–225.
- Romanczuk, P., Schimansky-Geier, L., 2012. Mean-field theory of collective motion due to velocity alignment. *Ecological Complexity* 10, 83–92.
- Rüdiger, S., 2014. Stochastic models of intracellular calcium signals. *Physics Reports* 534 (2), 39–87.
- Schultheiss, P., Cheng, K., 2012. Finding food: outbound searching behavior in the australian desert ant *melophorus bagoti*. *Behavioral Ecology* 24 (1), 128–135.

- Schulze, C., Stauffer, D., 2005. Monte carlo simulation of the rise and the fall of languages. *International Journal of Modern Physics C* 16 (05), 781–787.
- Seeley, T. D., 1989. The honey bee colony as a superorganism. *American Scientist* 77 (6), 546–553.
- Simpson, M. L., Cox, C. D., Allen, M. S., McCollum, J. M., Dar, R. D., Karig, D. K., Cooke, J. F., 2009. Noise in biological circuits. *Wiley Interdisciplinary Reviews: Nanomedicine and Nanobiotechnology* 1 (2), 214–225.
- Simpson, S. J., Sword, G. A., 2008. Locusts. *Current Biology* 18 (9), R364–R366.
- Sotiropoulos, V., Kaznessis, Y. N., 2011. Analytical derivation of moment equations in stochastic chemical kinetics. *Chemical engineering science* 66 (3), 268–277.
- Spector, L., Klein, J., Perry, C., Feinstein, M., 2005. Emergence of collective behavior in evolving populations of flying agents. *Genetic Programming and Evolvable Machines* 6 (1), 111–125.
- Strogatz, S. H., 2018. *Nonlinear dynamics and chaos: with applications to physics, biology, chemistry, and engineering*. CRC Press.
- Strömbom, D., 2011. Collective motion from local attraction. *Journal of theoretical biology* 283 (1), 145–151.
- Sumpter, D. J., 2006. The principles of collective animal behaviour. *Philosophical Transactions of the Royal Society of London B: Biological Sciences* 361 (1465), 5–22.
- Sumpter, D. J., 2010. *Collective animal behavior*. Princeton University Press.
- Toner, J., Tu, Y., 1995. Long-range order in a two-dimensional dynamical xy model: how birds fly together. *Physical review letters* 75 (23), 4326.
- Torney, C. J., Levin, S. A., Couzin, I. D., 2010. Specialization and evolutionary branching within migratory populations. *Proceedings of the National Academy of Sciences* 107 (47), 20394–20399.
- Traulsen, A., Claussen, J. C., Hauert, C., 2012. Stochastic differential equations for evolutionary dynamics with demographic noise and mutations. *Physical Review E* 85 (4), 041901.
- Uvarov, B., 1977. *Grasshopper and locust: a handbook of general acridology*. vol. ii: Behaviour, ecology, biogeography. *Population Dynamics* (Cambridge Univ. Press, Cambridge, 1977).
- Van Kampen, N. G., 1992. *Stochastic processes in physics and chemistry*. Vol. 1. Elsevier.
- Vicsek, T., Czirók, A., Ben-Jacob, E., Cohen, I., Shochet, O., 1995. Novel type of phase transition in a system of self-driven particles. *Physical review letters* 75 (6), 1226.
- Wang, Z., Bauch, C. T., Bhattacharyya, S., d’Onofrio, A., Manfredi, P., Perc, M., Perra, N., Salathé, M., Zhao, D., 2016. Statistical physics of vaccination. *Physics Reports* 664, 1–113.
- Wood, A. J., Ackland, G. J., 2007. Evolving the selfish herd: emergence of distinct aggregating strategies in an individual-based model. *Proceedings of the Royal Society of London B: Biological Sciences* 274 (1618), 1637–1642.
- Yates, C. A., Erban, R., Escudero, C., Couzin, I. D., Buhl, J., Kevrekidis, I. G., Maini, P. K., Sumpter, D. J., 2009. Inherent noise can facilitate coherence in collective swarm motion. *Proceedings of the National Academy of Sciences* 106 (14), 5464–5469.

Yuan, Y., Allen, L. J., 2011. Stochastic models for virus and immune system dynamics. *Mathematical biosciences* 234 (2), 84–94.